Master's Thesis in Environmental Engineering

Adsorption of Per- and Polyfluoroalkyl Substances (PFASs) on Granular Activated Carbon: A Column Study

By

Narges Moghadasi

Supervisor:
Prof. Ranjandrea Sethi
Co-Supervisor:
Francesca Nunzio

Politecnico di Torino
2025

Declaration

I hereby declare that the contents and organization of this dissertation constitute my own original work and does not compromise in any way the rights of third parties, including those relating to the security of personal data.

Narges Moghadasi

2025

* This dissertation is presented in partial fulfillment of the requirements for **master's degree** at Politecnico di Torino.

Acknowledgment

First and foremost, I would like to express my deepest gratitude to my supervisor, **Professor Sethi**, for his invaluable guidance, support, and encouragement throughout the course of this research. I am also sincerely thankful to my advisor, **Francesca Nunzio**, for her thoughtful advice and continuous support. My heartfelt thanks go to all the colleagues at the **Clean Water Center at Politecnico di Torino**, Luca Purice, Dr. Monica Grannetto, and Marco Coha whose collaboration and assistance made this work possible.

Finally, I am profoundly grateful to my beloved **husband**, my **family**, and my **friends**, whose unwavering love and encouragement were a constant source of strength during the most challenging times.

Abstract

The research investigates the water treatment capabilities of fixed-bed granular activated carbon (GAC) columns for removing perfluorobutanoic acid (PFBA), perfluorobutanesulfonic acid (PFBS), perfluorooctanoic acid (PFOA), and perfluorooctane sulfonic acid (PFOS) from water. PFASs are considered emerging pollutants because they have been widely used and persist in the environment while posing risks to ecosystems and human health. The research evaluates chemical adsorption at low environmental concentrations through simulations of real-world contamination to address increasing regulatory focus and drinking water PFAS occurrences.

The research starts by reviewing PFAS characteristics and their health and environmental impacts as well as global drinking water regulatory limits and existing treatment solutions. Granular activated carbon adsorption represents a primary treatment method for PFASs because it offers efficient performance at affordable prices. The research included a brief assessment of previous column studies to support experimental planning. The first stage of research evaluated the potential release of PFAS compounds from materials used in column configurations. The adsorption behavior of each chemical was studied individually on a sand bed before performing competitive adsorption experiments on GAC. HPLC-MS/MS was used to analyze experimental data. The research findings enhance our knowledge about PFAS-GAC adsorption mechanisms which will help develop better treatment systems for contaminated water.

Keywords: PFASs; Granular Activated Carbon (GAC); Competitive Adsorption; Column Test

Contents

List of Figures

List of Tables

Chapter 1

1. Introduction

The water crisis, encompassing water quality, is one of the top ten global challenges, and both human activities and climate change at regional and national levels impact water quality (W. Yuan et al., 2023). With the intensification of climate change, issues such as prolonged droughts, changing precipitation patterns, and increased frequency of extreme weather events further threaten the availability and reliability of clean water resources, making the provision of safe and high-quality water more critical than ever. With over 9000 compounds, poly- and perfluoroalkyl substances (PFASs) are a complex group of anthropogenic organic pollutants that are known to repel water, oil, and stains. They are distinguished by a special molecular structure that includes a chain of fluorinated carbon atoms, which makes them incredibly resistant to environmental degradation. Since the 1950s, they have been used all around the world in a variety of commonplace items, including firefighting foams, kitchenware, clothing, carpets, and food packaging. Because of their exceptional resistance to photolytic, chemical, and biological destruction, PFASs survive in the environment for long stretches of time. Furthermore, the sulfonate or carboxylate groups make PFASs more hydrophilic, which improves their environmental mobility and transit (Behnami et al., 2024; Dirani, Ayoub, Malaeb, & Zayyat, 2024).

PFASs have extremely little adsorption by soils or aquifers, and surface and groundwater readily carry them into the environment. Due to their extremely stable and migratory nature, PFAS easily move from the source site to surface water or groundwater. They have been found in many water sources worldwide and have been demonstrated to have contaminated groundwater in residential areas and public drinking water systems (ATSDR, 2021). Because groundwater is a source of drinking water in many parts of the world, PFAS pollution of groundwater is significant. Therefore, drinking tainted groundwater can expose people and animals to PFAS. PFAS contain fluorine atoms bonded to a carbon atom chain; the carbon chain length and functional head group vary depending on the desired chemical properties. The distinctive and advantageous chemical characteristics of PFAS are based on the carbon–fluorine link, which is the strongest and shortest covalent chemical bond in nature. The degree of difficulty in remediating PFAS can also be influenced by their length and functional head group.

Because of their long history of use and established toxicological effects, two "long-chain" perfluorinated compounds—perfluorooctanoic acid (PFOA) and perfluorooctane sulfonic acid (PFOS)—have received most of the regulatory attention to date, even though there are thousands of different PFAS compounds. Shorter chain length PFAS have typically gotten less attention than PFOA and PFOS, but the sudden and recent discovery of these compounds in drinking water and wastewater sources has sparked interest in learning more about their potential toxicological effects as well as remediation strategies. According to convention, compounds with less than seven perfluorinated carbon atoms are classified as short-chain perfluoroalkyl carboxylic acids, while those with fewer than six perfluorinated carbon atoms are classified as short-chain perfluoroalkyl sulfonic acids (Westreich, Mimna, Brewer, & Forrester, 2018).

Over 60% of all perfluorocarboxylate emissions are caused by chemical releases from the production of fluoropolymers, both in the air and in industrial waste. Additional causes include the usage and disposal of Aqueous Film-Forming Foams (AFFFs), emissions from reapplication to carpets or textiles, landfill leachate from abandoned items and packaging, and wear from the textile and carpet industries. PFASs may be released into the land, water, and air by these sources. Based on their physicochemical characteristics, the chemicals—particularly the end-product PFASs—are likely to accumulate and move through water resources because they rarely stay in the gaseous state and because the adsorption of soil, sediments, and sludges is anticipated to be restricted. Some populations living close to fluoropolymer production sites have elevated levels of exposure to PFOA, PFOS, and other perfluoroalkyls because of contaminated drinking water (Steenland et al., 2009).

The sustainability of agriculture in Europe is seriously threatened by PFAS pollution, especially in areas that are close to industrial areas or use intensive farming methods. Trudel et al. suggested that the main ways that the public in Europe and North America is exposed to PFOS are through the consumption of food and water, dust ingestion, and hand-to-mouth transmission from mill-treated carpets, based on environmental observations and theoretical models (Valalamontes & Adamopoulos, 2025; Vestergren, Cousins, Trudel, Wormuth, & Scheringer, 2008). International and national legislation have designated long-chain PFAS, which are hazardous and bioaccumulative. According to toxicological studies, PFASs have a variety of detrimental impacts on human health, such as hepatotoxicity, effects on reproduction and development, neurotoxicity and endocrine toxicity, cardiovascular disorders, renal effects, and immunological effects (ATSDR, 2021).

A growing number of state regulatory agencies have established or proposed regulatory limits for PFOA and PFOS at or below the USEPA's health advisory to safeguard the public, and several of those agencies have also included guidelines on short-chain PFAS. Provisional lifetime health recommendations for PFOA and PFOS in drinking water were updated by the U.S. Environmental Protection Agency (USEPA) in May 2016 from 0.4 micrograms per liter (µg/L) and 0.2 µg/L, respectively, to a combined concentration of 0.7 µg/L (USEPA, 2016a). The purpose of health advisories is to inform public water system operators about the possible

harmful health effects of exposure to dangerous chemicals, even if they are not legally binding or regulated.

By January 12, 2026, the European Union requires adherence to parametric values of 0.5 µg/L for PFAS total (sum of all PFAS) and 0.1 µg/L for the sum of 20 PFAS, as outlined in Directive 2020/2184. A growing number of state regulatory agencies have established or proposed regulatory limits for PFOA and PFOS at or below USEPA's health advisory to safeguard the public. Furthermore, a growing number of public drinking water systems are concerned about other PFAS chemicals and are concentrating on voluntarily treating non-detect levels of PFOA and PFOS. Many parties in charge of PFAS-contaminated locations are working to address remediation operations in order to remove any potential liability for drinking water pollution (Westreich et al., 2018).

Because the PFAS cannot be completely removed by conventional wastewater treatment methods, they pass through the treatment process and are eventually released into water bodies. Because of its strong C–F bond, which makes it difficult to break down through the ordinary oxidation process, PFAS has a high chemical resilience (Rahman, Peldszus, & Anderson, 2014). Thus, it is necessary to investigate the effectiveness of sophisticated physical separation techniques like adsorption and high-pressure membranes. Granular activated carbon (GAC) and other adsorption technologies have become popular and practical ways to remove PFAAs from low levels of contamination. Previous studies have shown that GAC effectively eliminates long-chain PFAS but less effectively eliminates short-chain PFAS (Ochoa-Herrera & Sierra-Alvarez, 2008; Senevirathna, Tanaka, Fujii, Kunacheva, Harada, Shivakoti, et al., 2010). Despite GAC's quick discovery of short chain PFAS, its simplicity of use, low cost per unit of media, and reliable adsorption of PFAS and co-contaminants have made it one of the most widely used technologies for treating PFAS-contaminated groundwater.

A relatively high dose of PFAS, ranging from high micrograms per liter (µg/L) to milligrams per liter (mg/L), spiked into water has been used in most of the published experimental research on PFAS removal. These values are not typical in aquatic habitats, where levels of PFAS typically range from low µg/L to low nanograms per liter (ng/L). To assess the effectiveness of granular activated carbon (GAC) for PFAS removal, this study used column experiments to examine four PFAS compounds as representative analytes: PFOS and PFOA (long-chain), PFBS and PFBA (short-chain), which are frequently found in water sources under environmentally relevant concentrations and conditions.

Because column experiments are quicker, more flexible, and less expensive than in-depth field research, we aimed to assess the adsorption of the GAC in PFASs removal using column test. Column experiments can produce accurate estimations of important transport parameters and permit controlled boundary conditions. One major obstacle, nevertheless, is creating standardized column techniques for researching the behavior of organic micropollutants. There are three primary sequential phases to this investigation. Four distinct PFAS chemicals are examined for possible release or adsorption from the materials utilized in the column setup in the

first phase. The behavior of PFASs in sand medium at low concentrations is assessed in the second phase. In the last stage, a combination of the four chosen PFAS compounds is used in column tests to investigate the competitive adsorption of PFASs on granular activated carbon (GAC) which is a common challenging condition in PFAS contaminated sites or aquatic ecosystems (Domingo & Nadal, 2019). Finally, the adsorption behavior of PFBA on GAC was studied, as the removal of short-chain PFAS compounds remains hard due to their poor affinity for adsorbents like GAC, which is frequently employed in treatment procedures for its cost-effectiveness (Li et al., 2023).

Following this introductory section, the thesis is organized into four main chapters. Chapter 2 presents a comprehensive literature review. It begins with an overview of PFASs, including their definitions, classifications, physicochemical properties, regulatory limits, and toxicological impacts. The chapter then explores various PFAS remediation technologies, with a particular focus on GAC-based adsorption and the underlying mechanisms. It concludes with a review of previous studies on PFAS removal using GAC in column experiments. Chapter 3, *Materials and Method*, outlines the experimental design and methodologies employed in this research. It includes the characterization of sand and GAC, evaluation of PFAS release and adsorption from setup materials, tracer and transport testing, and the use of HYDRUS-1D for modeling hydraulic and reactive transport parameters. Chapter 4, *Results* and Chapter 5 *Conclusion*, presents the outcomes of this experimental work and summarizes the key findings of the study and offers recommendations for future research.

Chapter 2

2. Literature Review

2.1 What are PFASs?

Thousands of synthetic organic compounds belonging to the PFAS family are distinguished by linear or branching carbon-fluorine chains that are joined to a functional group. EPA defined PFAS using the following technical definition for the Multi-Industry PFAS Study: Per- and polyfluorinated compounds with the structural unit R-(CF2)-C(F)(R')R", where all the R groups (R, R', or R") cannot be hydrogen and both the CF2 and CF moieties are saturated carbons ((EPA), 2021). The majority of the 5000–10,000 molecules that make up PFAS are extremely resistant to breaking down in the environment under normal conditions, which is why they are known as "forever chemicals."(Habib, Song, Ikram, & Zahra, 2024). PFAS gives materials non-stick, heatproof, and waterproof qualities; as a result, they are used in a variety of consumer goods, including furniture, cleaning supplies, and non-stick cooking equipment. The Organization for Economic Co-operation and Development (OECD) updated its definition of PFAS in 2021 to include fluorinated compounds with at least one completely fluorinated alkyl component, such as an aromatic ring, methyl (-CF3), or methylene carbon atom (-CF2-). There are a few exceptions, though, such as those totally fluorinated alkyl moieties that do not have any H, Cl, Br, or I atoms attached. Over 7 million PFAS chemical species are known to exist worldwide, and their numbers are continually rising, according to the PubChem Classification. The toxicity of perfluoroocatanesulfonic acid (PFOS) and perfluorooctanoic acid (PFOA), the two PFAS with the longest production histories, has been extensively studied. Consequently, the Stockholm Convention has added PFOA, its salts, and related compounds, PFHxS, and related substances, PFOS, its salts, and perfluorooctane sulfonyl fluoride (PFOSF) to the list of new persistent organic pollutants (POPs) (Buck et al., 2011; Leung, Wanninayake, Chen, Nguyen, & Li, 2023).

2.2 PFASs Properties

High polarity and inert carbon-fluorine (CF) bonds provide PFAS with its persistence, high heat stability, and chemical stability. Because of these characteristics, it is difficult to control their presence in many environmental compartments, such as soil, water, and air. Understanding the distinct chemical structure of PFAS is a prerequisite for analyzing their physical interactions. A perfluorinated chain (tail) and a functional group (head) are the two primary constituents of all PFAS variations. A perfluorinated chain (Rf) is basically an alkyl chain with a head that can be carboxylate or sulfonate with all the hydrogen atoms swapped out for fluorine atoms. The distinct physical and chemical characteristics of PFAS are attributed to their perfluorinated tail. Since fluorine is the most prevalent element in PFAS, as the word "perfluorinated" implies, and since its atomic structure plays a significant role in determining the chemical and physical properties of PFAS, it is crucial to first briefly discuss fluorine's features.

2.2.1 Properties of fluorine

The type of fluorine and the quantity of strong C–F bonds in their structure are the main factors influencing the special physicochemical characteristics of PFAS. Fluorine has a low polarizability, a high ionization energy, and an exceptionally high electronegativity. With bond dissociation energies in PFAS as high as 531.5 kJ mol^{-1}, fluorine, the most electronegative element in the periodic table, forms one of the strongest and most chemically inert single bonds with carbon. Because of this, PFAS are much more stable chemically and physically than their hydrocarbon counterparts (Leung et al., 2023).

2.2.2 Chemical properties

Because of the optimum orbital overlap between the carbon orbitals in the C–F bonds and the fluorine's 2s and 2p orbitals, PFAS demonstrate exceptional stability and produce various dipolar resonance structures along the perfluoroalkyl chain. The more fluorine atoms that are connected to a core carbon, the stronger the C–F bond. The three lone pairs on each fluorine atom, along with their partial negative charges, create steric and electrostatic shields around the core carbon atom in perfluorinated compounds like CF_4. By shielding the carbon center from nucleophilic attack, this shielding helps to maintain the kinetic stability of PFAS. A major contributing factor to PFAS's chemical inertness is this structural characteristic.

The C–F bond is strongly polarized due to fluorine's high electronegativity. The bond's electrons gravitate toward fluorine (δ−), while the carbon remains electropositive (δ+) due to sp^3 hybridization. The polarization energy of the bond is further enhanced by fluorine's short atomic radius. Furthermore, PFAS's ionic nature is influenced by fluorine's poor polarizability, which also produces a stronger link than its hydrocarbon counterparts. The strong electron-withdrawing inductive effect of the perfluoroalkyl chain can both decrease the basicity of organic bases and

greatly raise the acidity of functional groups like alcohols. The hyper-conjugative stabilization seen in β-fluorination, which is indicated by a discernible drop in pKa when a fluorine atom replaces a hydrogen atom in the alkyl chain, is also connected to this increase in acidity. Fluorine is a poor acceptor of hydrogen bonds due to its low electron polarizability, even though it has lone electron pairs and a high electronegativity (Kirsch, 2006; Krafft & Riess, 2015; Leung et al., 2023).

2.2.3 Physical properties

Fluorine, whose greater van der Waals radius introduces steric hindrance, replaces hydrogen atoms to give PFAS their distinctive structural characteristics. As a result, the carbon backbone undergoes notable structural changes, including a twisted helical structure that differs from the zigzag pattern found in hydrocarbons. Because of these modifications, PFAS molecules become less conformationally flexible and stiffer. They have less conformational freedom than their hydrocarbon counterparts, as evidenced by their trans/gauche entropy, which is roughly 25% higher.

Because of fluorine's low polarizability, PFAS also show weak intra- and intermolecular interactions, which leads to lower boiling temperatures and higher volatility when compared to related hydrocarbons. Surface wettability is increased by this weak interaction's oleophobic nature and low surface tension. Despite the polarized C–F bonds, PFAS has a nonpolar, hydrophobic property due to its amphiphilic structure and internal dipole moment cancellation. PFAS can thus form a separate phase by separating from both polar and non-polar solvents.

PFAS often have a lower critical micelle concentration (CMC) than hydrocarbons, which is a crucial metric for environmental transport and cleanup. The reason for this is that CF_2 units have a micellization energy that is roughly 1.5 times greater than CH_2. Longer fluorinated chains in fluorinated surfactants have higher surface activity, which also improves solubilization at low doses. Counterions have an impact on surface activity, but it is negligible in comparison to chain length. At room temperature, fluorinated surfactants are limited to chains of C7–C8, though, because longer chains raise the Krafft point. Fluorinated surfactants form smaller micelles than their hydrocarbon counterparts. Micelle size and shape are influenced by the amount of salt present in the surrounding medium; with high salt concentrations, long-chain PFAS form rod-like micelles, whereas short-chain PFAS often form ellipsoidal micelles. By lessening the repulsion between anionic headgroups, higher salt concentrations also decrease CMC. A significant environmental concern is the bioaccumulation potential of PFAS, which is controlled by CMC, vapor pressure, and water solubility. Longer-chain PFAS are more likely to bioaccumulate because of the interdependence of these characteristics: boiling point has an inverse relationship with vapor pressure and a positive correlation with solubility and CMC (Bhhatarai & Gramatica, 2011; Leung et al., 2023).

2.3 PFASs Classification

The chemical and physical characteristics, behavior, and possible hazards to human health and the environment of PFAS vary greatly. Individual PFAS differ in their chemical structure, length of carbon chain, degree of fluorination, and chemical functional group or groups. These differences affect the PFAS's mobility, fate, and degradation in the environment as well as its uptake, metabolism, clearance, and toxicity in plants, animals, and humans. A lot of PFAS are resistant to heat, water, and oil, have a low surface tension, and are chemically and thermally stable. These characteristics make PFAS beneficial in a variety of industrial processes and consumer goods, but they also make them persistent in the environment. The fluorine atom's tiny size, strong electronegativity, low polarizability, and the strength of the carbon-fluorine covalent bond are the main causes of PFAS's distinctive and appealing properties. The two most often utilized methods for producing PFAS are electrochemical fluorination and fluorotelomerization. Until analytical techniques became commercially available in the 2000s, PFAS were not extensively recorded in environmental samples, despite being produced and utilized in several sectors both domestically and abroad since the 1940s. Since then, analytical techniques for detecting PFAS at lower concentrations and for various environmental media and PFAS compounds have been regularly developed. PFAS are now widely found in the environment, biota, and people, as well as in isolated places all over the world. Non-polymers and polymers are the two categories into which the hundreds of compounds that comprise the PFAS family can be separated. There may be groups, subgroups, and subclasses within each class. The PFAS classes and groups are depicted in Figure 1((EPA), 2021), ((ITRC), 2023), (Ferndahl, 2024).

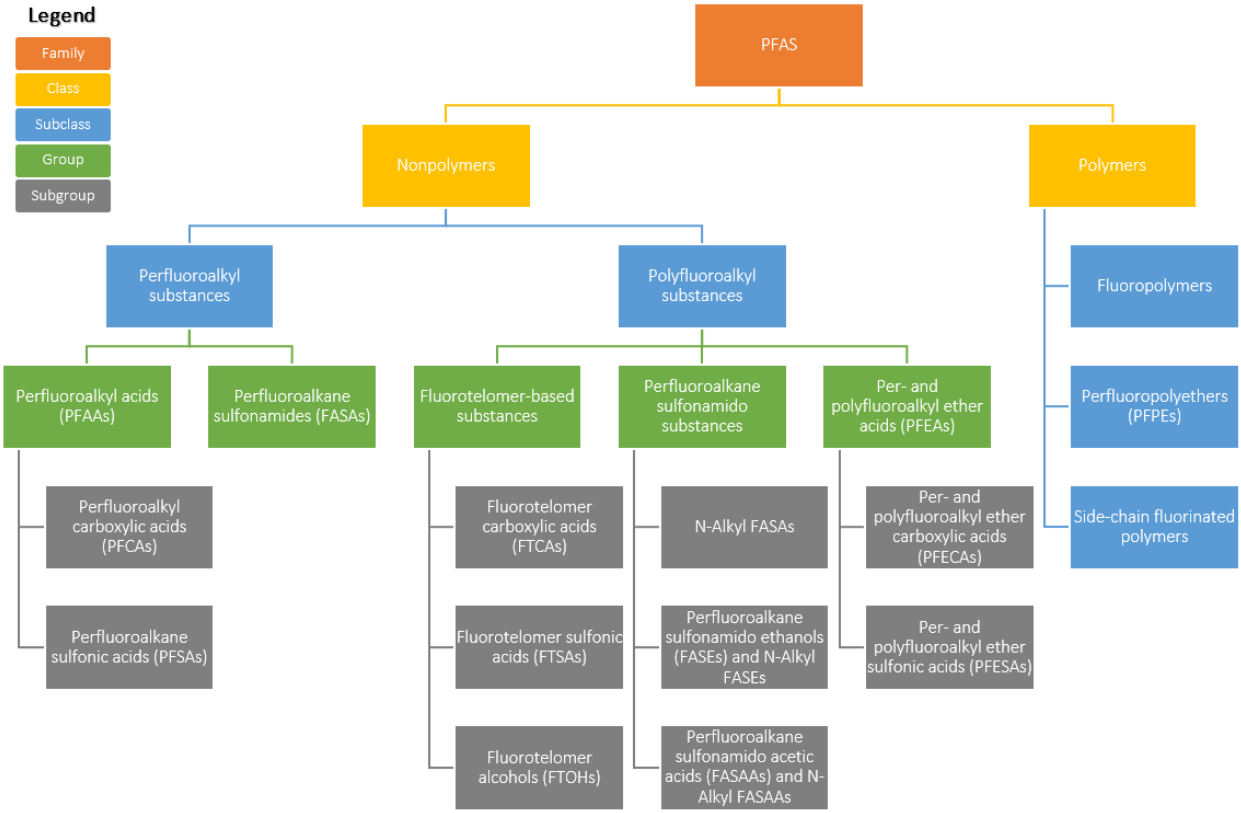

Figure 1. PFAS classes and groups

2.3.1 Non-polymer PFAS

Perfluoroalkyl substances (totally fluorinated carbon chain) and polyfluoroalkyl substances (partially fluorinated carbon chain) are two subclasses of the non-polymer PFAS class that comprise different chemical groups and subgroups.

2.3.1.1 Perfluoroalkyl Substances

Fully fluorinated alkane molecules with a charged functional group (head) and a tail of two or more carbons are known as perfluoroalkyl compounds. The most common PFAS compounds to be detected in the environment are PFAAs (Perfluoroalkyl Acids), which are also the simplest. PFAAs are the end products of the breakdown of more complex PFAS (precursors) and do not break down in the environment. PFCAs (Perfluoroalkyl Carboxylic Acids) and PFSAs (Perfluoroalkyl Sulfonic Acids) are the two primary subgroups of PFAAs. Whereas PFSAs can only be produced by electrochemical fluorination, PFCAs can be produced by either electrochemical fluorination or fluorotelomerization. The number of carbons covalently linked to fluorine determines whether PFAAs are categorized as long-chain or short-chain. Eight or more carbons make up long-chain PFCAs (seven or more of which are perfluorinated), while six or more carbons make up long-chain PFSAs (six or more of which are perfluorinated). Because one

carbon in the PFCA molecule is linked to the functional group rather than the fluoroalkyl tail, PFCAs behave more like seven-carbon PFSAs than eight-carbon PFSAs in terms of chemical behavior. This is because PFCAs are more similar to PFSAs with one extra carbon than PFSAs with the same number of carbons. PFAAs with longer chains do not break down spontaneously into those with shorter carbon-fluorine chains ((ITRC), 2023; Ferndahl, 2024). Figure 2 and Figure 3 show the molecular structure of the long chain and short chain PFASs used in the current study.

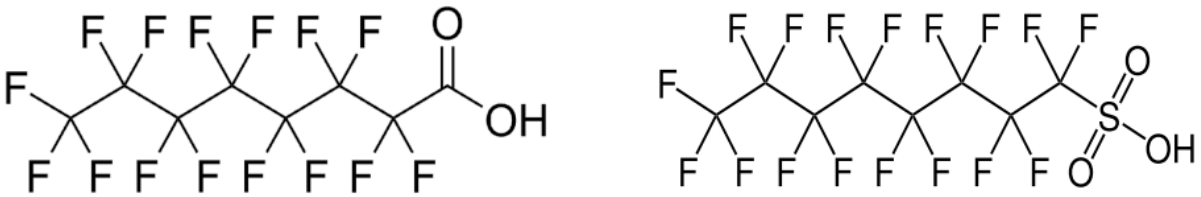

Figure 2. Molecular structures of PFOA (left) and PFOS (right) ((EPA), 2021)

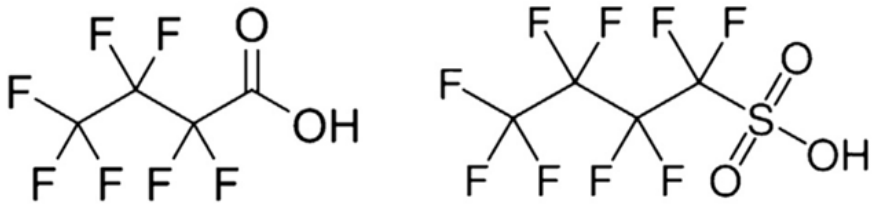

Figure 3. Molecular structures of PFBA (left) and PFBS (right) (Appleman, Dickenson, Bellona, & Higgins, 2013)

2.3.1.2 Polyfluoroalkyl Substances

One characteristic that sets polyfluoroalkyl compounds apart is their incomplete fluorination. Instead, two or more of the remaining atoms in the carbon chain tail are fully fluorinated, whereas at least one carbon atom—usually hydrogen or oxygen—has a nonfluorine atom connected to it. Numerous PFAS have the potential to change into PFAAs because the nonfluorinated link in polyfluoroalkyl compounds creates a weak point that is prone to degradation. Fluorotelomer-based compounds, perfluoroalkane sulfonamido substances, and per- and polyfluoroalkyl ether acids (PFEAs) are the three categories of polyfluoroalkyl substances. Fluorotelomer-based compounds are created through fluorotelomerization and are named

according to the x:y convention, in which x denotes the number of carbon atoms that are fully fluorinated and y denotes the number of carbon atoms that are not.

Although they are not seen to change into PFSAs, compounds based on fluorotelomers have the potential to be PFCA precursors. Fluorotelomer alcohols (FTOHs), fluorotelomer sulfonic acids (FTSAs), and fluorotelomer carboxylic acids (FTCAs) are the three subgroups. In addition to having a fully fluorinated tail, perfluoroalkane sulfonamido compounds have one or more methylene (CH2) groups in the head of the molecule that are joined to the sulfonamido spacer. Electrochemical fluorination produces perfluoroalkane sulfonamido compounds, which can break down into PFCAs and PFSAs. Perfluoroalkane sulfonamido ethanols (FASEs), perfluoroalkane sulfonamido acetic acids (FASAAs), and N-alkyl FASAs are the three subgroups. PFEAs, which include per- and polyfluoroalkyl ether carboxylic acids (PFECAs) and per- and polyfluoroalkyl ether sulfonic acids (PFESAs), are produced by fluorotelomerization. Long-chain PFAAs like PFOA and PFOS are being phased out, and several PFECAs and PFESAs have been created to replace them. Hexafluoropropylene oxide dimer acid (HFPO-DA), 4,8-dioxa-3H-perfluorononanoic acid (DONA) and its ammonium salt (ADONA), and chlorinated PFESAs are the PFEAs that are receiving the most interest ((EPA), 2021).

2.3.2 Polymer PFAS

Large molecules called polymer PFAS are created by repeatedly joining numerous identical smaller molecules, or monomers. Non-polymer PFAS may be discharged during incineration or degradation, utilized as raw materials or processing aids in the production of certain polymer PFAS, or included as impurities in polymer products. Side-chain fluorinated polymers, fluoropolymers, and perfluoropolyethers (PFPEs) are the three subclasses of polymer PFAS. The backbone of a fluoropolymer is a carbon-only polymer to which fluorine is directly bonded. Non-polymer PFAS have been employed as processing aids in the polymerization of some fluoropolymers, but they are not usually manufactured from non-polymer PFAS raw materials. A few high-molecular-weight fluoropolymers, such as ethylene tetrafluoroethylene (ETFE) and polytetrafluoroethylene (PTFE), are less bioavailable, insoluble in water, and chemically and thermally stable. According to available data, these fluoropolymers are thought to be less harmful to human and environmental health than non-polymer PFAS because their molecules are too big to pass through cell membranes. The backbones of perfluoropolyethers (PFPEs) are carbon and oxygen polymers, to which fluorine is directly bonded. PFPEs are generally insoluble in water and are thought to possess chemical and thermal stability. Long-chain PFAAs or their possible precursors are not used to make PFPEs, nor are they a component of their production. Fluorinated side chains break off of a nonfluorinated polymer backbone in side-chain fluorinated polymers. When the fluorinated side-chain's point of attachment to the polymer is damaged, some may break down into PFAAs ((ITRC), 2023; Ferndahl, 2024).

2.4 PFASs Applications and Use

Because of its unique characteristics, PFAS are used in a wide range of applications. Since at least the 1950s, they have been utilized in consumer, business, and industrial settings for products like firefighting foams, textile coatings, surfactants, food contact materials, and pesticides (Gaines, 2023). Additionally, they can be found in makeup removers, hand sanitizers, and hair care products. Another significant use of PFAS is water-repellent apparel, which contains fluorotelomer alcohols (FTOHs), perfluorinated carboxylic acids (PFCAs), and perfluoroalkyl sulfonic acids (PFSAs). PFAS have been found in a variety of products, including food contact materials (FCMs), outdoor clothing, carpeting, carpet cleaners, floor waxes, and upholstery, because of its use in multiple applications. In humid environments, PFAS can effectively be applied as an anti-mist coating on the surface of plastic, glass, and metals to prevent blurring or fogging, which is common in toilets, car windshields, and eyeglass lenses. PFAS may be utilized as surfactants to boost well oil and gas recovery rates (Gaines, 2023), (Habib et al., 2024).

2.5 PFASs Main Sources

Point and non-point sources are the main sources of PFAS in the environmental compartments. While diffuse sources of unknown location or origin primarily refer to non-point sources, such as degradation precursor compounds, precipitation, surface runoff, and atmospheric intrusion of volatile PFAS, point sources are stationary and discrete and include landfills, firefighting training facilities, wastewater treatment units, manufacturing, and industrial amenities (Habib et al., 2024).

2.6 PFASs Related Health Effects

The main way that people are exposed to PFASs is through contaminated drinking water. Human exposure to PFAS has several detrimental impacts on health. Numerous detrimental consequences on fetuses, neonates, toddlers, adolescents, and adults have been documented in studies (Kumara & Bhattacharyya, 2022). Figure 4 shows the possible health effects induced by PFASs exposure in adults and children.

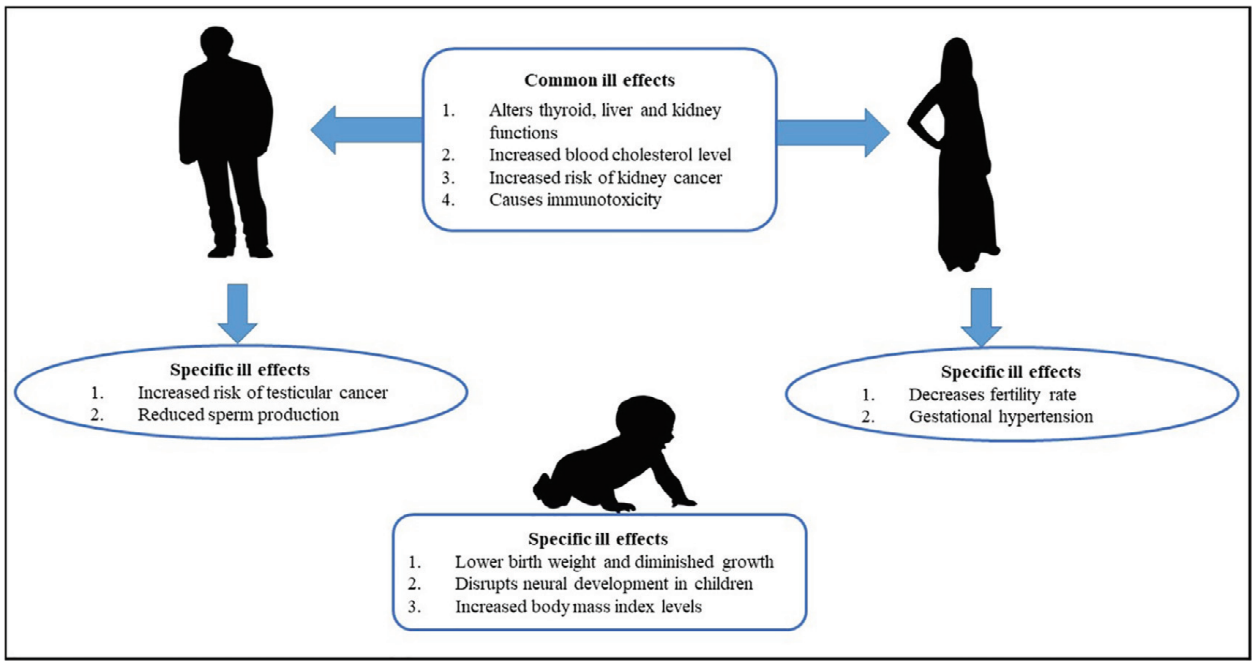

Figure 4. Health effects of PFASs exposure among humans (Kumara & Bhattacharyya, 2022)

The elimination rate of PFASs in women is correlated with the chemicals' half-life, age, menstruation status, childbearing, and nursing. Due to its ability to pass across the placental barrier, PFAS exposure during pregnancy causes changes in the size and development of the fetus's brain. In the detected range of 0.22–30.3 µg/L in serum and 0.16–6.68 µg/L in blood proteins, neonatal exposures to PFAS can cause eczema, pneumonia, respiratory syncytial virus infection, wheezing, asthma, and chickenpox. When children are exposed to PFASs, their immunity is weakened. Research at measured levels of PFASs ranging from 18.4 to 31.3 µg/L has shown decreased antibody production to vaccines (meant to resist rubella, measles, and mumps). Exposure to PFASs impacts thyroid, kidney, and liver function. Since the liver is the main organ that long-chain PFASs target, PFASs build up there. They raise the amount of lipids in human blood and cause poisoning. Increased blood levels of Gamma-Glutamyl Transferase (GGT), Alanine Aminotransferase (ALT), Aspartate Aminotransferase (AST), and bilirubin are markers of liver damage linked to PFAS exposure (Kumara & Bhattacharyya, 2022).

Chronic kidney disease is brought on by PFASs in the blood, which lowers glomerular filtration. As a result, blood uric acid levels rise. By attaching themselves to thyroid hormones that transport proteins, PFASs have an impact on the circulation of Thyroxine (T4) levels. In humans, PFASs lead to breast, ovarian, and testicular cancer. Studies have reported the prevalence of breast cancer among women under 50 years. Exposure to PFAS causes changes in sex hormone levels, estrogen secretion, menarche delay, and menstrual cycle disruption in women. Although short-chain PFASs are homologs of established long-chain PFASs, researchers

have observed their uptake by food crops and may bioaccumulate. Since short-chain PFASs will be used more frequently in the ensuing decades, research on their environmental fate during the early phases of manufacture helps prevent negative effects. Additionally, the goal should be to produce substitutes that, when released into the environment, may totally decompose with little to no negative impact. Additionally, this will lessen the usage of current PFAS in the majority of applications (ATSDR, 2021; Kumara & Bhattacharyya, 2022)

The following illnesses and health outcomes were deemed to be sufficiently associated by the Committee on the Guidance on PFAS Testing and Health Outcomes in the USA: Dyslipidemia in adults and children, reduced antibody response in adults and children, and possible health effects of PFAS a higher chance of kidney cancer in adults, as well as impaired growth in infants and fetuses. The following illnesses and health outcomes were determined to have little or suggestive evidence of a link by the committee: The evidence was scant, insufficient, or limited for a variety of other health impacts. Type 1 and gestational diabetes; cardiovascular disease; metabolic syndrome; obesity; infertility; male and female reproductive effects; reproductive hormone levels; cancers other than kidney, breast, and testicular; increased risk of breast cancer in adults; liver enzyme changes in adults and children; increased risk of pregnancy-induced hypertension (gestational hypertension and preeclampsia); increased risk of testicular cancer in adults; increased risk of thyroid disease and dysfunction in adults; and increased risk of ulcerative colitis in adults (National Academies of Sciences & Medicine, 2022).

2.7 PFASs Regulatory Threshold Limits in Water

To mitigate PFAS pollution, much more work needs to be done. There is mounting evidence that PFAS are harmful to both the environment and human health. Government rules must be in place to restrict the discharge of PFAS chemicals into the environment to safeguard the aquatic ecosystem. Globally, strict new rules have started to be implemented. Many nations or international expert agencies are beginning to implement regulatory measures to protect drinking water, establishing limit values for PFAS and requiring testing and monitoring, as drinking water is becoming one of the major sources of PFAS exposure. Although PFAS pollution is a worldwide problem, many countries have different management and remediation strategies and laws.

2.7.1 Europe

Two PFAS indicators are outlined in the European Union's (EU) updated Drinking Water Directive 2020/2184 (later DWD): The parameter is the "Sum of PFAS" that contain a perfluoroalkyl moiety with three or more carbons (i.e., –CnF2n-, n > 3) or a perfluoroalkylether moiety with two or more carbons (i.e., –CnF2nOCmF2m-, n and m > 1) with a parametric value of 0.1 µg/L. "PFAS total" refers to the totality of PFAS, which has a parametric value of 0.5

μg/L. But according to DWD Annex III, "These substances shall be monitored when the risk assessment and risk management of the catchment areas for abstraction points are carried out and conclude that these substances are likely to be present in a given water supply." Moreover, it is not necessary to monitor these compounds until January 2026 (Directive, 2020).

As several EU Member States have done in the case of PFAS limitations and monitoring, the DWD's criteria serve as a minimum that they must adhere to but are not precluded from enacting domestic laws that are more comprehensive or strict. Some EU Member States have set stricter drinking water levels than those required by DWD, basing their national drinking water standards on the European Food Safety Authority (EFSA) view while implementing the new EU drinking water regulations. Following the EFSA opinion, the following national criteria and advisory values apply to the "Sum of 4 PFAS": Belgium and Sweden (4×10^{-3} μg/L), Denmark (2×10^{-3} μg/L), the Netherlands (4.4×10^{-3} μg/L, PFOA equivalents), Germany (2×10^{-2} μg/L), and Spain (7×10^{-2} μg/L) (Kozisek et al., 2025).

In Italy, the regulation of per- and polyfluoroalkyl substances (PFAS) in water is governed by both national and regional laws, aligning with European Union directives. Legislative Decree 6 July 2016 transposes the European Directive 2014/80/EU, amending Annex II of Directive 2006/118/EC, with a focus on protecting groundwater against pollution. The threshold values for the assessment of the chemical status of the groundwater, which includes the five PFASs; Perfluoro pentanoic acid (PFPeA), Perfluorohexanoic acid (PFHxA), Perfluorooctanoic acid (PFOA), Perfluorooctysulphonic acid (PFOS) are respectively 3 μg/L, 1 μg/L, 3 μg/L, 0,5 μg/L, and 0,03 μg/L (*Legislative Decree 6 July 2016, No. 122: Transposition of EU Directive 2014/80/EU amending Annex II of Directive 2006/118/EC*, 2016). Regarding drinking water, Legislative Decree 18/2023 implements the EU Directive 2020/2184 concerning the quality of water intended for human consumption. It sets 0.1 μg/L for total PFAS and 0.5 μg/L for the sum of 20 specified PFAS (Government, 2023).

Data from the European Environment Agency (EEA) indicate that PFOS contamination in northern Italy is a widespread issue, with many surface water monitoring sites registering levels exceeding the Environmental Quality Standard (EQS) of 0.00065 μg/L. As shown in Figure 5, in several locations, concentrations exceed this benchmark by factors ranging from 10 up to more than 100. A similar trend is observed in groundwater, particularly in urbanized and industrial areas, where PFOS concentrations frequently exceed the national limit of 0.03 μg/L, as defined by the Italian Legislative Decree of July 2016. By contrast, the southern regions of the country generally exhibit lower levels of PFOS, with most readings remaining within the acceptable thresholds set by both national and EU regulations ((EEA), 2024). The contamination is particularly noticeable in Piedmont, which is toward the northwest. The region's surface water testing frequently shows PFOS levels significantly higher than the EQS. Several sites have shown amounts between 0.01 and 1 μg/L in groundwater measurements, which again exceeds permissible limits. These findings highlight Piedmont's industrial development's environmental

legacy and support the justification for Regional Law 25/2021, which forbids the introduction of PFAS into shallow groundwater and soil and places stringent restrictions on emissions. The concentration limitations for PFOS, PFOA, PFBA, and PFBS are 0.00065 µg/L, 0.10 µg/L, 7 µg/L, and 3 µg/L, respectively, according to this law (Piemonte, 2021).

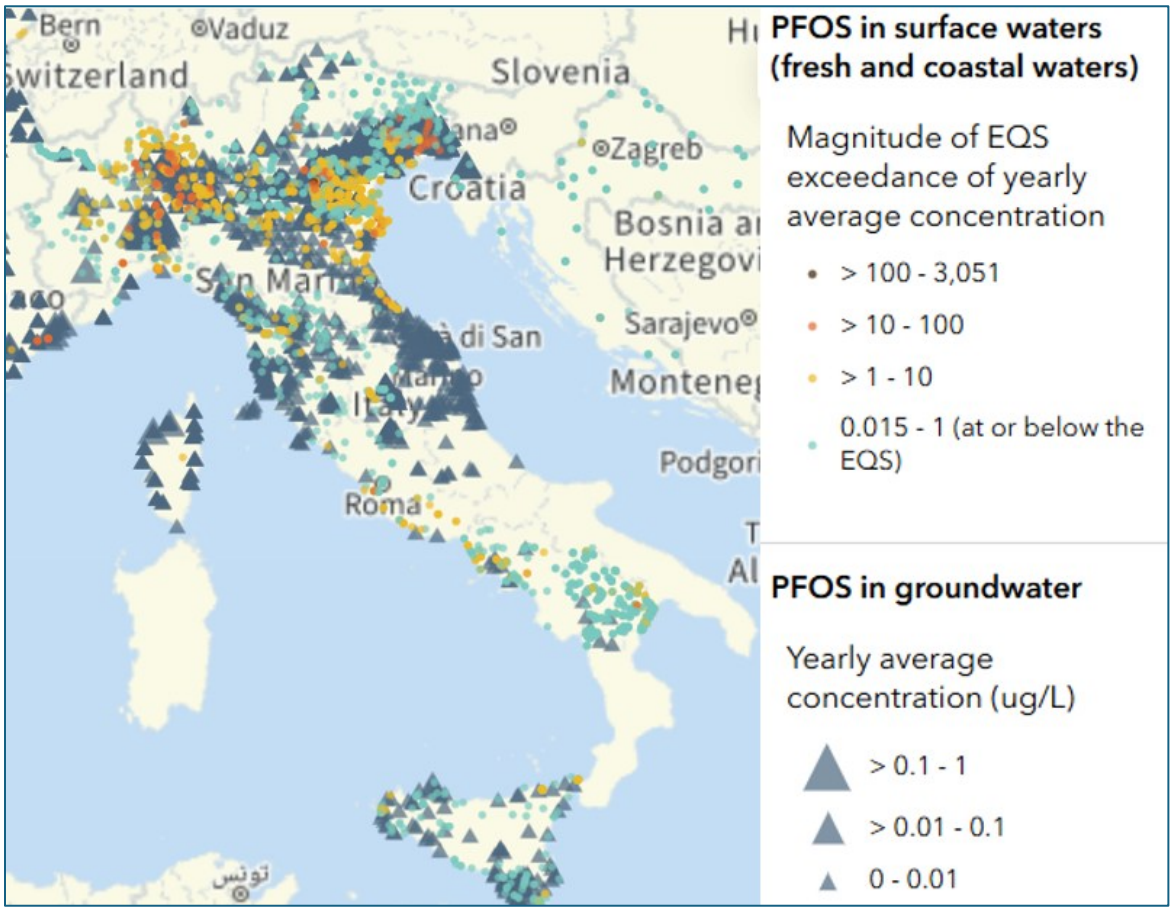

Figure 5. PFOS level in groundwater and surface water in Italy

2.7.2 United States and North America

In An important milestone in federal environmental regulation was reached in 2024 when the U.S. Environmental Protection Agency (EPA) adopted the first nationally enforceable drinking water limits for per- and polyfluoroalkyl substances (PFAS). Perfluorooctanoic acid (PFOA) and perfluorooctane sulfonic acid (PFOS) have maximum contamination limits (MCLs) of 4×10^{-3} µg/L under the Safe Drinking Water Act, whereas PFHxS, PFNA, GenX (HFPO-DA), and PFBS are controlled using a cumulative hazard index method. All public water systems are required to adopt these standards by 2029, after which they must be monitored by 2027. The requirement for standardized national limitations and growing concern about the health effects of PFAS are reflected in this regulatory framework (Agency, 2025).

A national target for PFAS in drinking water has been recommended by Health Canada, which suggests that the combined content of the 25 known PFAS compounds not surpass 0.03 µg/L. This guideline, which is presently being reviewed, would signify a change from regulating specific PFAS compounds to a comprehensive strategy based on PFAS (Canada, 2024).

2.7.3 Australia, Africa, and Asia

The Australian Drinking Water Guidelines (Version 3.9) state that the combined concentration of PFOS and PFHxS should not be greater than 0.07 µg/L, while the health-based guideline value for PFOA in drinking water is 0.56 µg/L. Food Standards Australia New Zealand's (FSANZ) risk evaluations serve as the foundation for these levels ((Australia), 2011).

Africa lacks legally binding, continental-wide drinking water regulations for PFAS as of 2025. The urgent need for thorough regulatory frameworks is shown by the numerous studies that have documented PFAS contamination in several African nations. Weak enforcement measures and the illegal importation of products containing PFAS exacerbate the widespread prevalence of PFAS in the environment (Umejuru, Street, & Edokpayi, 2024).

Most Asian nations have significant regulatory gaps and no specific PFAS legislation. According to a survey analysis encompassing 12 Middle Eastern and Asian nations, there is no specific PFAS water regulation in place (Tang, Hamid, Yusoff, & Chan, 2023). However, as of 2019, Korea's drinking water quality monitoring standard for perfluorinated chemicals has been set at 0.07 ug/L for PFOA, 0.48 µg/L for PFOS, and 0.07 µg/L for PFHxS (Hong et al., 2024). Taiwan has drafted enforceable standard of 0.05–0.07 µg/L for selected PFAS, to take effect in 2027. Vietnam and China have identified PFAS as priority pollutants, with regulatory frameworks currently under development (Ji, 2024; Lee, Smaoui, Duffill, Marandi, & Varzakas, 2025; Senevirathna, Tanaka, Fujii, Kunacheva, Harada, Shivakoti, et al., 2010).

2.8 Treatment Technologies for PFASs Removal

PFAS can be eliminated via separation or oxidation. Electrocoagulation, advanced oxidation process, ozonation, thermal destruction, biodegradation, sonochemical/ultrasound, plasma treatment, microwave hydrothermal treatment, and vapor energy generator are some of the oxidation techniques. Reactive oxygen species can cause the PFAS chemicals to decompose into smaller molecules during the oxidation process. However, oxidation techniques for PFAS removal are costly, complicated, and energy-intensive to operate. On the other hand, adsorption ion exchange, nanofiltration, reverse osmosis, and membrane filtration are among the separation techniques that are extensively researched to eliminate PFAS. By combining additional

procedures, the separation method can create a multi-barrier strategy that improves treatment effectiveness overall. The efficiency of the degrading process can be impacted by the concentration of PFAS, the length of the PFAS chain, and the presence of additional contaminants or coexisting ions (Jais et al., 2024).

2.9 PFASs Adsorption on Granular Activated Carbon

One important technique for treating water is adsorption technology, which provides a quick, affordable, and adaptable way to recycle and purify water. It entails the accumulation of chemicals on a solid phase in order to separate them from a fluid phase (Fath & Jorgensen, 2020). Granular activated carbon (GAC) is a kind of carbonaceous sorbent made from carbonaceous inputs like wood, coal, or coconut shells that are chemically or thermally activated to generate a highly porous structure. The physicochemical properties of GAC are influenced by its source ingredients, activation processes, and post-activation treatments, which in turn affect its adsorption capacities (Crincoli, Jones, & Huling, 2020). GAC can be thermally regenerated, has been used for decades to treat drinking water, and has been shown to be successful in eliminating PFASs. Now, it is the most practical PFAS control technique for drinking water treatment facilities. The GAC treatment effect of PFASs is unknown since the influent water quality that the GAC process encounters frequently varies while the full-scale drinking water treatment plants (DWTPs) are operating. Numerous factors, such as carbon age, influent flow rate, carbon properties, PFAS hydrophilicity/hydrophobicity, pH, ionic strength, and organic matter present in the bulk water, have been shown to affect the GAC's PFAS adsorption capacity (Jais et al., 2024).

2.9.1 Adsorption Mechanism on GAC and Affecting Factors

Hydrophobic, electrostatic, and hydrogen bonding interactions are typically a part of the adsorption mechanism. Numerous elements pertaining to the PFAS compounds themselves, the properties of the GAC, and the water chemistry all affect how well PFASs adsorb onto granular activated carbon (GAC). These elements may have an impact on GAC's effectiveness and ability to remove PFAS from water treatment procedures. One important aspect influencing PFAS's adsorption onto GAC is its hydrophobicity. Research indicates a relationship between the hydrophobicity of PFAS, measured by Log K_{ow} (octanol-water distribution coefficient), and the half breakthrough bed volume (BV50), a measure of adsorption capacity. PFAS have a stronger affinity for the hydrophobic surfaces of activated carbon since their Log K_{ow} values tend to rise with the length of their carbon chains. Because of these advantageous interactions with the non-polar areas of the GAC surface, long-chain PFAS often show higher adsorption than shorter-chain PFAS. The anionic functional group of PFAS and the charged GAC surface interact

electrostatically. These interactions are also influenced by the chemistry of the background solution, such as pH and ion composition. While hydrophobic interactions mostly govern the adsorption of long-chain PFAS on GAC, electrostatic interactions dominate the adsorption of relatively hydrophilic short-chain PFAS. Carboxylic acids (-COOH) and sulfonic acids ($-SO_3H$), which are common charged functional groups found in PFASs, easily ionize at ambient pH conditions to produce negatively charged species. These PFAS are primarily found in their protonated, neutral form at low pH levels (acidic environments). They deprotonate and acquire a negative charge as the pH rises. However, GAC surfaces typically show amphoteric activity, which means that depending on the pH of the solution, they can acquire either positive or negative charges. The pH at which the GAC surface has a net zero charge is known as the point of zero charge (pH_{pzc}). The GAC surface has a positive charge below the pH_{pzc} and a negative charge above it. The GAC surface gains a net positive charge when the pH of the solution falls below the pH_{pzc}, which makes it easier for negatively charged PFAS anions to be attracted to it. For the elimination of PFAS over a larger pH range, activated carbons with higher pH_{pzc} values are therefore thought to be more effective. PFAS adsorption is influenced by additional GAC properties such as origin, porosity, and number of reactivations, large surface area and pore volume, surface chemistry, and chemical modification (Zhiyuan Liu et al., 2024; Pan et al., 2019; Zhang, Thomas, Apul, & Venkatesan, 2023).

The qualities of groundwater or drinking water can also have an impact on adsorption efficiency. Other important factors include water temperature, flow rate, dissolved organic matter (DOM), ionic composition, and the presence of other microorganisms. Dissolved organic matter (DOM), ionic composition, and other microorganism contamination might change the surface charge of GAC or compete with PFASs for GAC adsorption sites. However, because active sites gradually become saturated, GAC's adsorption capability tends to decrease with time. Further adsorption is limited, and its efficacy is diminished as PFAS molecules build up on the surface and produce electrostatic repulsion against other anions in solutions.

Furthermore, it is stated that raising the water's temperature will speed up the discovery of perfluoroalkyl carboxylic acids (PFCAs). Conversely, lower flow rates typically result in longer contact times and better adsorption (Belkouteb, Franke, McCleaf, Köhler, & Ahrens, 2020; Nakazawa, Kosaka, Yoshida, Asami, & Matsui, 2023; Siriwardena et al., 2019).

2.10 Column Test

An effective technique for evaluating the efficacy and efficiency of different adsorbent materials for pollutant removal under settings that closely resemble real-world applications is column testing, also known as fixed-bed column studies. These tests offer a more realistic depiction of continuous water treatment processes, which is helpful for improving the design of water treatment systems. They also simulate continuous flow conditions and offer important insights into the dynamic behavior of adsorbents and their potential for real-world use in water purification processes. Adsorbent material is placed into a column, and water containing the

target contaminant is constantly delivered through the column. Over time, the contaminant's concentration in the effluent—the water that leaves the column—is tracked. A breakthrough curve is created using this data, which is essential for assessing the effectiveness of the adsorbent. Adsorbent capacity, breakthrough behavior, and the impact of different operating parameters can all be assessed by column studies.

A standard column test configuration includes several essential elements: 1) A reservoir of contaminated water that holds the water that needs to be treated and has a known concentration of the target pollutant, 2) Pump: utilized to supply the column with tainted water at a regulated flow rate. Because of its accuracy in regulating flow, peristalsis pumps are frequently utilized. 3) Column: an adsorbent material-filled cylindrical tube. The height and diameter of the column is crucial measurements. 4) Sampling ports: these allow water samples to be taken at various depths throughout the column to track the treatment process and the last step 5) is effluent collection, which involves gathering treated water from the column for analysis. A breakthrough curve, which is a plot of the effluent concentration vs time or volume of water treated, is created using the data collected from the measurement of the pollutant concentration in the effluent over time. It offers crucial details regarding the adsorption column's performance. The adsorbent is said to be at its saturation point when the effluent concentration hits a predefined threshold. The adsorbent is fully saturated at the exhaustion points where the effluent concentration equals the influent concentration. Adsorption capacity, or the total amount of pollutants removed by the adsorbent, is represented by the area under the breakthrough curve. Several variables can affect how well adsorption columns work: Flow Rate: Early breakthrough curves may result from shorter contact times between the contaminant and the adsorbent caused by higher flow rates. Influent Concentration: Adsorbent saturation may occur more quickly with higher influent concentrations. Bed Depth: Adding more adsorbent to the bed can increase treatment capacity and postpone breakthrough. The performance of an adsorbent is greatly influenced by its type, particle size, surface area, and chemical characteristics. pH: Adsorption can be impacted by the water's pH and temperature.

2.10.1 Recent Column Test Studies for PFASs Removal from Water

To identify the optimal configuration and experimental condition in column test, some critical variables that were considered in the previous PFAS removal column test studies which used granular activated carbon are reported in Table 1.

Table 1. Recent column studies on PFAS removal using GAC

Reference study	Column material	PFASs Concentration	Flowrate	Tested water	Experiment Condition/Duration	Sampling Interval	Column Dimension/Bed	Adsorbent
(Appleman et al., 2013)	Glass	1 µg/L of each PFASs	1 mL/min	Deionized water	Up-flow, 33 days	Influent: once per week Effluent: every 3–4 days	D: 7 mm, filled with 1cm GAC, a layer of glass beads and glass wool	GAC, 0.21 mm
(Senevirathna, Tanaka, Fujii, Kunacheva, Harada, Ariyadasa, et al., 2010)	Polypropylene (PP)	PFOS 10 µg/L	--	Tap water	Downflow mode, columns effluent approached 0.2 C0 which took about 60 days.	Effluent of each column was collected periodically 1 L from each column	L: 30 cm, D: 2 cm, filled with 20 cm3 of adsorbent	GAC, 0.25–0.5 mm
(Chularueangaksorn, Tanaka, Fujii, & Kunacheva, 2014)	Polypropylene (PP)	PFOA 5 µg/l	15 ml/min	Tap water	Down-flow mode, 117 days, when the PFOA removal efficiency of all of the columns reduced to 90%	Effluent: every three days.	L: 30 cm, D: 2 cm, filled with 20 cm3 of adsorbent	GAC, 0.25 to 0.50 mm
(Murray, Marshall, Liu, Vatankhah, & Bellona, 2021)	--	PFAAs 175 ppt-12500 ppt	46 mL/min	Tap water	Down-flow mode, 18 months	Influent twice a month	L:91 cm, Din:2.5 cm, 3 segments of GAC, each 27 cm	GAC, 0.42–1.68 mm

(J. Yuan, Mortazavian, Passeport, & Hofmann, 2022)	Glass	PFOA and PFOS 100 ng/L each	0.3 ml/min	Dechlorinated Drinking water spiked by PFASs	Down-flow mode, 25 h to 125 h depending on the EBCT, to ensure that a pseudo steady state was reached.	Periodically	L:30 cm, D:2.5 cm, two 10 cm layers of glass beads (1 mm in diameter), 10 cm GAC	10 cm GAC
(Kempisty et al., 2022)	PTFE	10 PFAAs 650 ng/L	EBCT 7.5 min	Groundwater	EBCT of 7.5 min	Every 3-4 days	D: 4.76 mm, filled with GAC, glass wool	GAC, 0.11 mm logarithmic mean diameter
(Liu, Peldszus, Sauvé, & Barbeau, 2024)	HDPE	ambient background PFAS contamination of samples	5 ml/min, EBCT 0.06 min	Filtered Drinking water and ozonated water	Up-flow mode, 4.2 days	--	D: 0.64 cm filled with 0.3 ml GAC+ 0.3 mL silica sand	GAC, 0.4-1.7 mm
(Cantoni, Turolla, Wellmitz, Ruhl, & Antonelli, 2021)	--	1 µg/L of each PFASs	0.29-0.34 L/hr (4.8-5.7 ml/min)	tap water	Up-flow mode, seven days	Influent: every 2 days, Effluent: every 3 hours	Diameter :7 mm, 190 mg sieved GAC + glass beads	GAC, 90–125 µm
(Niarchos, Ahrens, Kleja, & Fagerlund, 2022)	PVC	0.87 mg/l for 12PFASs,	288 mL/day (0.2 ml/min)	Artificial ground water	Up-flow, 150 days	Effluent: every 3 days	L:15 cm, D: 3.6 cm, 2 cm gravel Filled with 306 ± 1.7 g of dry soil (<2 mm) + premium 40/50 silica sand, GAC, 1–2 µm with final concentration of	GAC, 1–2 µm

							0.031% w/w	

Chapter 3

3. Materials and Method

3.1 PFASs Solutions

The four PFASs, two long-chain and two short-chain were selected for the analysis. Their main characteristics are reported in Table 2. The single and mixture solutions were prepared in deionized water produced by Milli-Q water purification system, by diluting standard solutions in glass bottles. Before injection the solutions were degasified. The pH of the solutions was around 6.5.

Table 2. Chemical characteristics of experiment PFASs

Molecule	Molecular weight (gr/mol)	pK_a	$logK_{ow}$
PFBS (*Perfluorobutane sulfonic acid)*	300	0.14	3.9
PFBA (*Perfluorobutanoic acid)*	214	0.4	2.82
PFOS (*Perfluorooctane sulfonic acid)*	500	-3.27	6.43
PFOA (*Perfluorooctanoic acid)*	414	-0.2	5.3

3.2 Characterization and Evaluation of Materials for Column Packing

Before performing any test, the main physical and chemical characteristics of the material used for the column test were measured. The D8 sand used for packing was a medium silica sand (Dorsilit 8, Dorfner, Germany) with particle sizes d10 = 0.415 mm, d50 = 0.45 mm, and d90 = 0.5 mm. To ensure a stable configuration and proper flow distribution at the top and bottom of the column, a coarse silica sand (Dorsilit 5G, Dorfner, Germany) with particle sizes d10 = 1.12 mm, d50 = 1.58 mm, and d90 =1.9 mm was employed. A commercial granular activated carbon, named Carbopur 1240 produced by Brenntag S.p.A, Italy was employed as an adsorbent. Its main properties are reported in Table 3.

Table 3. Properties of commercial GAC

Property	Value
Iodine number	950 mg/gr
pH	alkaline
Density	490 ± 10 kg/m^3
Particle size	12x40 mesh
Hardness	95%
Humidity	5%
Ash content	15%

3.2.1 Characterization of the GAC

The physical and chemical properties of the selected GAC were measured and reported by master student *Iris Barbero*, who investigated the adsorption of these four PFASs on the GAC performing the kinetic and isothermal experiments. The following procedures were carried out for this purpose (Barbero, 2024).

3.2.1.1 Elemental Composition

Using the Scanning Electron Microscope (SEM), the elemental composition of both washed and unwashed AC was examined. A drop of the GAC grains was applied to the sample container using double-sided carbon tape after first creating a suspension

of the grains in deionized water. The washed and unwashed GAC samples were characterized using this final method. The sample's particle sizes had to be reduced using a ceramic mortar and pestle prior to making the two suspensions of the appropriate types of activated carbon in deionized water. Then, for a few minutes, the two sample containers containing the drops of the washed and unwashed activated carbon solutions were placed in an oven set to 50 $^{\circ C}$ to dry.

Both samples were then prepared for the SEM analysis using the "Q 150R S" automatic sputter coater. This apparatus enables the examined elements to interact with the electron flow of the SEM by encasing the samples in gold. Several measurements were made using the SEM attached to the "EDAX Genesis" detector, and various sample sections were subjected to microanalysis using the "xT microscopic control" program.

Images captured by SEM of the unwashed and washed activated carbon (AC) sample are shown in

Figure 6 and Figure 7, respectively. Spots that were considered for microanalysis are indicated by the red letters. Table 4 and Table 5 show the weight and atomic percentage findings of the microanalysis in each of the six locations together with the calculated mean values for unwashed AC. The measured data show that the impurity level is low and restricted to a trace amount of oxygen and silicium, which are frequently found in ashes. On the contrary, the preparatory coating that was done before the SEM study is responsible for the appearance of gold in specified areas.

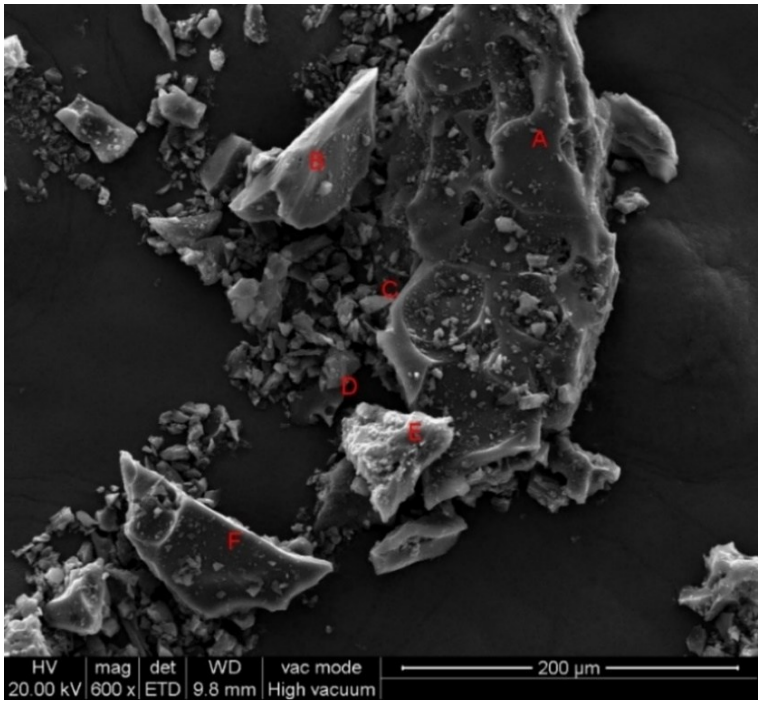

Figure 6. SEM measure of unwashed AC

Table 4. Weight percentages of the 6 spots (A, B, C, D, E, F) of measure of unwashed AC

	Wt (%) C	**Wt (%) O**	**Wt (%) Al**	**Wt (%) Si**	**Wt (%) Au**
A	95.57	0	0	0	4.43
B	94.85	0	0	0	5.15
C	88	7.56	0	1.34	3.1
D	95.86	0	0	1.61	2.53
E	88.82	3.34	2.68	5.16	0
F	94.26	0	0	0	5.74
Mean	92.89	1.82	0.45	1.35	3.49

Table 5. Atomic percentages of 6 spots (A, B, C, D, E, F) of measure on unwashed AC

	At (%) C	At (%) O	At (%) Al	At (%) Si	At (%) Au
A	99.72	0	0	0	0.28
B	99.67	0	0	0	0.33
C	93.18	6.01	0	0.61	0.2
D	99.13	0	0	0.71	0.16
E	93.76	2.65	1.26	2.33	0
F	99.63	0	0	0	0.37
Mean	97.51	1.44	0.21	0.61	0.22

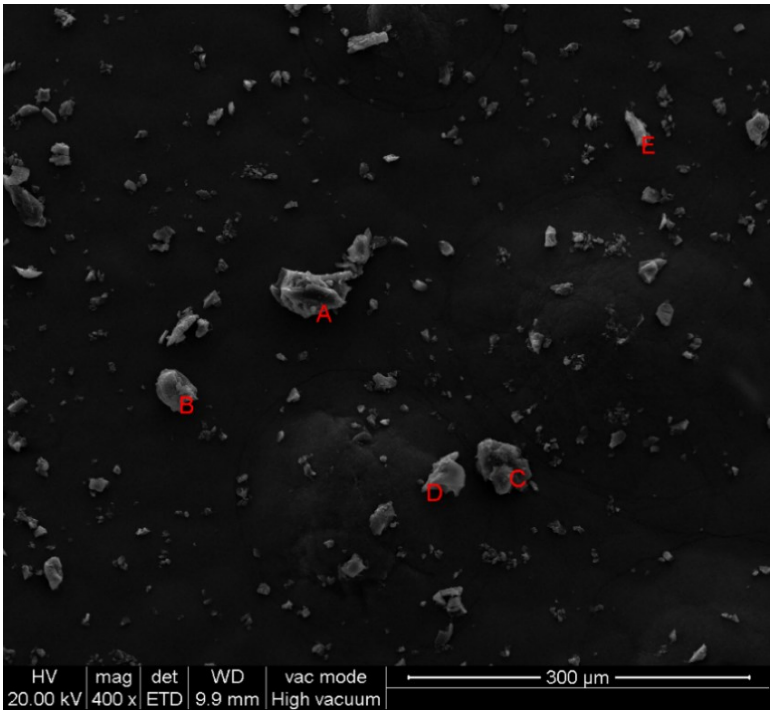

Figure 7. SEM measure of washed AC

Table 6. Weight percentages of 6 spots (A, B, C, D, E) of measure of washed AC

	Wt (%) C	**Wt (%) O**	**Wt (%) Al**	**Wt (%) Si**	**Wt (%) Au**
A	95.58	0	0	0	4.42
B	95.3	0	0	0.75	3.95
C	97.08	0	0	2.92	0
D	100	0	0	0	0
E	90.02	7.36	0	0	2.62
Mean	95.60	1.47	0	0.73	2.20

Table 7. Atomic percentages of 6 spots (A, B, C, D, E) of measure of washed AC

	At(%) C	**At (%) O**	**At (%) Al**	**At (%) Si**	**At (%) Au**
A	99.72	0	0	0	0.28
B	99.41	0	0	0.34	0.25
C	98.73	0	0	1.27	0
D	100	0	0	0	0
E	94.06	5.77	0	0	0.17
Mean	98.38	1.15	0	0.32	0.14

Table 7 and Table 7 present the findings related to the microanalysis of the washed AC.

As can be seen from the weight percentages, the unwashed AC has 92.9% carbon, while the washed AC has 95.6% carbon. This variance might be assumed to be related to the washing process, which oversees eliminating certain pollutants, resulting in a greater carbon percentage. The findings indicate that the weight percentage of silica was cut in half. Its content was 1.4% in the unwashed AC and 0.7% in the washed model. The oxygen content also dropped, going from 1.8% to 1.4%. The amount of carbon in the AC "as is" is equivalent to 97.5% of its atomic mass, but the amount in the washed AC is 98.4%.

3.2.1.2 Total Carbon

After identifying the elemental composition of the given GAC, the goal was to measure the total amount of carbon present in the activated carbon.

Several activated carbon samples, both washed and unwashed, were taken into consideration to conduct these tests. A TOC analyzer was used to ascertain their total carbon content. This device consists of a CO_2 detector that measures the amount of carbon dioxide present in the sample and a high temperature furnace that was set to 900 $^{\circ C}$ for the analysis. To relate the activated carbon samples' mass to their total carbon content, they were first weighed before being inserted into the TOC analyzer and sent for measurement.

The mean and standard deviations were calculated from the measurements of these tests. Table 8 reports the calculated results. Like the elemental analysis considerations, the removal of elements different from carbon through the washing process the sample had undergone is probably the reason why the washed AC has a slightly higher content of organic carbon and fewer contaminants.

Table 8. Total carbon in unwashed and washed AC

Sample	Concentration of Total Carbon (%)
Unwashed AC	80.78 ± 0.78
Washed AC	82.25 ± 0.42

3.2.1.3 Electrical Conductivity

To assess the electrical conductivity of both washed and unwashed activated carbon, four distinct samples—two with washed and two with unwashed activated carbon—were made. For each sample, approximately 0.04 L of deionized water (DIW) and 4×10^{-3} kg of activated carbon was combined to create a solution with the recommended 1:10 ratio, Table 9.

Table 9. Composition of the samples employed for the determination of the electrical conductivity

Sample	Unwashed AC (L of DIW, kg of AC)	Washed AC (L of DIW, kg of AC)
1	0.04 L, 4×10^{-3} kg	0.0432 L, 4.32×10^{-3} kg
2	0.04 L, 4×10^{-3} kg	0.0417 L, 4.17×10^{-3} kg

An orbital mixer was used to stir the four samples for an hour after they were placed in their respective Falcon tubes. The samples were then filtered through a PTFE membrane, and the electrical conductivity was determined by contacting the filtered solution with the conductivity electrode. TetraCon®325 was the conductivity probe model used for the measurement.

Table 10. Electrical conductivity of unwashed and washed AC

Sample	Unwashed AC Electrical Conductivity (µS/cm)	Washed AC Electrical Conductivity (µS/cm)
1	58	16
2	58	11

The unwashed activated carbon's electrical conductivity is equivalent to 58 µS/cm, while the washed activated carbon exhibits a decreased electrical conductivity of 15.5 ± 3.5 µS/cm, as anticipated. Electrical conductivity is known to correlate with the suspension's saline content, which in the case of the washed activated carbon was undoubtedly decreased by the washing process.

3.2.1.4 pH

First, a 0.01 mol/L solution of calcium chloride was made by adding 1.09×10^{-3} kg of CaCl2 ·6H2O (CAS No. 7774-34-7, Carlo ERBA Reagents, Italy) to 0.5 L of deionized water to measure the pH of the GAC. Then, four samples were made, two replicates of washed activated carbon and two replicates of activated carbon in its original form with the ratio 1:5, Table 11. The suspensions were combined for one hour in overhead mode after the four samples were placed in matching 0.05 L Falcon

tubes. The pH meter probe (pH 7 VIO with XS 201 T electrode, Italy) was then placed directly in contact with the fluids.

Table 11. Composition of the samples employed for the determination of pH of GAC

Sample	Unwashed AC (L of $CaCl_2$, kg of AC)	Washed AC (L of DIW, kg of AC)
1	25.55×10^{-3} L, 5.10×10^{-3} kg	25×10^{-3} L, 5×10^{-3} kg
2	26.4×10^{-3} L, 5.28×10^{-3} kg	27.75×10^{-3} L, 5.57×10^{-3} kg

Table 12. pH value of different washed and unwashed AC

Sample	Unwashed AC pH	Washed AC pH
1	11.13	10.78
2	11.19	10.81

It was found that pH values of the unwashed and washed activated carbon were respectively equal to 11.6 ± 0.042 and 10.8 ± 0.021.

3.2.1.5 Bulk Density

The bulk density was measured using a graduated cylinder. Inserting a specific mass of activated carbon into the cylinder and tapping the base and sides to even out the sample distribution inside the column. By dividing the mass by the observed volume occupied by the activated carbon, the bulk density was obtained. The identical method was used three times for both washed and unwashed activated carbon.

The standard deviations and mean were computed; Unwashed activated carbon has a bulk density of 430 ± 12 kg/m^3 and it was 440 ± 5.77 kg/m^3 for the washed activated carbon.

3.2.1.6 Granulometric distribution of GAC

A granular analysis was performed to describe the granulometric composition of the activated carbon that was being studied. A vertical series of vibrating sieves, Figure 9 with meshes of decreasing size was used to pass a mass of activated carbon to separate the various granulometric fractions of the unwashed and washed AC samples. To create the granulometric curve, the total masses of activated carbon that were retained by the various sieves were then weighed and the cumulative masses were calculated. Since a particular granulometric fraction, usually characterized by reduced dimensions, is frequently used for the adsorption batch tests of PFAS onto activated carbon, it was also determined to characterize a sample of crushed activated carbon. Using the same process as was used for the GAC in its original form, it was first ground using a ceramic mortar and pestle before being sieved to create its granulometric distribution.

Following sieving, the measured mass values allowed for the reconstruction of the grading curves, which are shown in Figure 8, as well as the calculation of the cumulative percentage of the net passing mass.

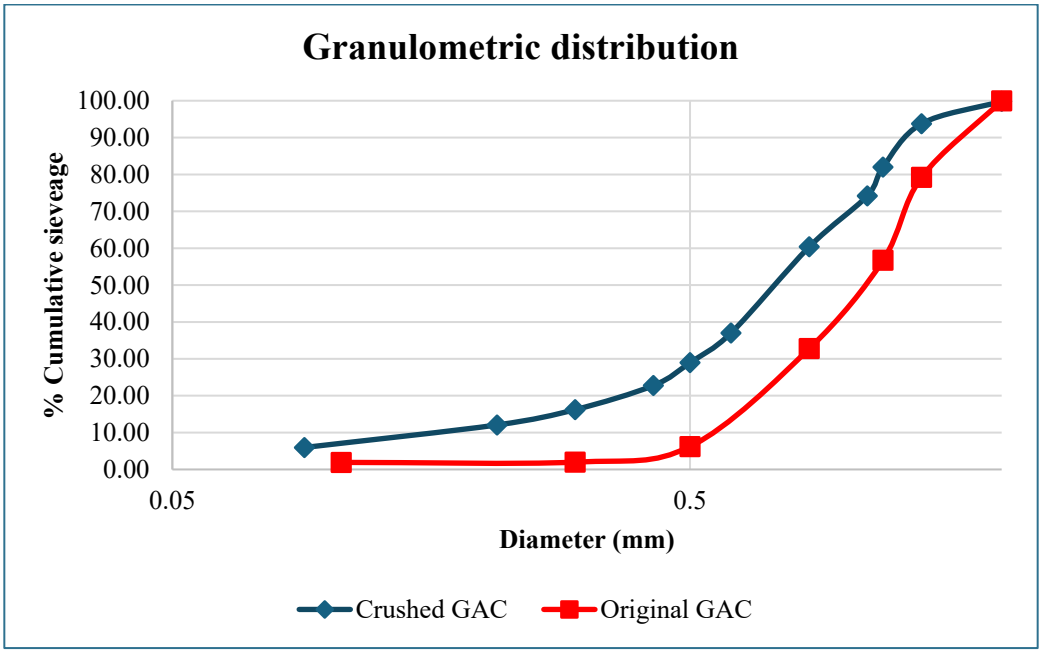

Figure 8. Comparison of the granulometric distribution between samples of original GAC and crushed GAC

A fraction with a diameter ranging from 0.425 mm to 0.85 mm was chosen based on the relative abundance of the granulometric fractions of the analyzed crushed activated carbon sample as well as the ranges of granulometric fractions typically chosen for the isotherm and kinetic adsorption batch tests. Figure 10 depicts the original GAC and crushed GAC samples.

Figure 9. Vertical series of vibrating sieves

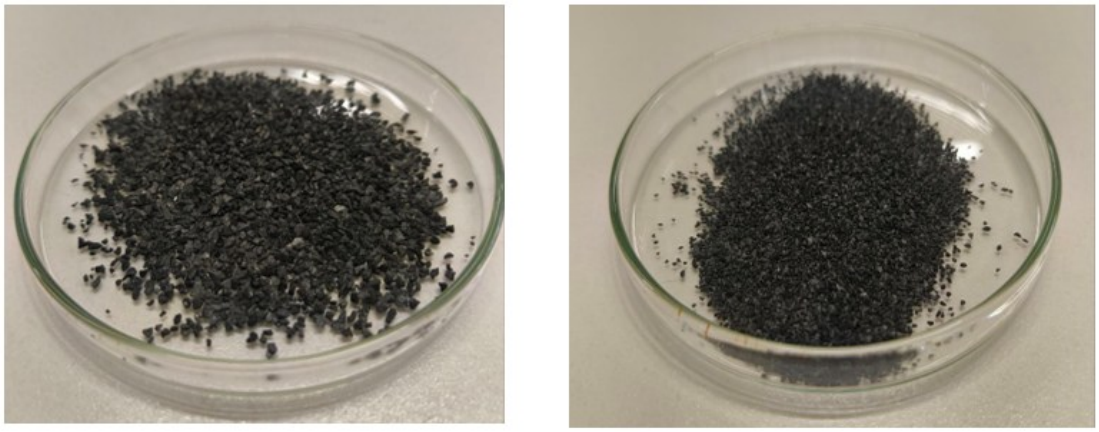
Figure 10. Original GAC (left) crushed GAC (right)

3.2.2 Characterization of Sand

Before packing the column, to remove all the particles and colloids adhering to the sand grains, using an ultrasonic bath, the sand was washed with tap water, soaked in deionized water overnight, and washed again several times with deionized water, NaOH 0.1 mol/L, and again deionized water. Then it was dried at 70 ^{oC} in the oven

(Memmert Universal Oven U, Gmbh, Germany) overnight. Some characteristics of the used sand were determined as follows:

3.2.2.1 Bulk Density

To measure the bulk density a graduated cylinder was used. A certain mass of sand was placed inside the cylinder, and the base and sides were tapped to ensure a uniform distribution of the sample. Then, the bulk density was calculated by dividing the mass by the measured volume occupied by the sand. This procedure was performed in triplicate for both unwashed and washed sand.

Table 13. Bulk density of washed and unwashed sand

Sample	No.	Bulk Density (kg/m^3)
Unwashed Sand	1	1530
	2	1530
	3	1530
Washed Sand	1	1570
	2	1540
	3	1550

The bulk density values for the samples are reported in the Table 13. The bulk density of the unwashed sand was found to be 1531 ± 3 kg/m^3. The bulk density of the washed sand was 1544 ± 13 kg/m^3.

3.2.2.2 Electrical Conductivity

To characterize the electrical conductivity of both washed and unwashed sand, four samples were prepared: two containing washed sand and two containing unwashed sand. Each sample was obtained by mixing approximately 4×10^{-3} kg of sand with 0.04 L of deionized water, achieving a 1:10 sand-to-water ratio.

The four samples were transferred into 0.05 L Falcon tubes and agitated using an orbital mixer for 1 hour. Then, the samples were filtered through a PTFE membrane filter, and electrical conductivity was measured by immersing the conductivity electrode into the filtered solution.

The measurements were performed using a TetraCon® 325 conductivity probe.

Table 14. Electrical conductivity of washed and unwashed sand

Sample	No.	Electrical Conductivity (μS/cm)	Temperature (°C)
Unwashed Sand	1	172	21.4
	2	176	21.6
Washed Sand	1	36	21.6
	2	38	21.4

The electrical conductivity of the unwashed sand was found to be 174 ± 2.82 μS/cm, whereas the washed sand showed a lower electrical conductivity of 37 ± 1.41 μS/cm, Table 14. This reduction in conductivity is related to the removal of dissolved salts and impurities during the washing process.

3.2.2.3 pH

First, a 0.01 mol/L solution of calcium chloride was made by adding 1.09×10^{-3} kg calcium chloride solution ($CaCl_2 \cdot 6H_2O$; CAS No. 7774-34-7, Carlo ERBA Reagents, Italy) was prepared by dissolving 1.0959 g of $CaCl_2 \cdot 6H_2O$ in 0.5 L of deionized water. Following the same procedure used for electrical conductivity measurements, four samples of sand were prepared: two replicates for washed sand and two replicates for unwashed sand. Five grams of each sample were added to separate 50 mL Falcon tubes, maintaining a 1:5 solid-to-liquid ratio by adding 0.025 L of the prepared solution, Figure 11.

Figure 11. Samples of unwashed (left) and washed sand (right)

The suspensions were then mixed for 1 hour using an overhead shaker. After mixing, the pH was measured by immersing the pH electrode directly into the solutions.

The pH of the washed and unwashed sand was determined to be 6.88 ± 0.014 and 6.84 ± 0.007, respectively, Table 15.
The comparison between washed and unwashed sand aimed to assess whether the washing process significantly alters the pH of the aqueous suspension, potentially due to the removal of dissolved minerals or surface contaminants. However, a minimal difference was observed.

Table 15. pH of washed and unwashed sand

Sample	No.	pH
Unwashed Sand	1	6.84
	2	6.85
Washed Sand	1	6.67
	2	6.89

3.3 Analytical Method for PFASs

The PFAS in the tested samples was analyzed using the HPLC-MS/MS method using the direct injection methodology. This method enables the highly sensitive and accurate detection of trace-level concentrations in accordance with the guidelines provided in the ASTM D7979 and EN 17892 standards. Because the direct injection

mode, often referred to as big volume injection, requires less sample preparation, it lowers the possibility of laboratory-induced PFAS contamination, which is a frequent problem in trace analysis. The technique makes use of isotope dilution analysis, Multiple Reaction Monitoring (MRM), and Negative Electrospray Ionization (ESI) to guarantee precise quantification and robustness in intricate sample matrices. Figure 12 illustrates the HPLC instrument used in this study for PFAS analysis.

Figure 12. UHPLC system coupled with a QTOF mass spectrometer used for PFAS analysis

3.4 Release of PFAS from the Different Materials in Column Test Setup

Before performing the actual column test, to assess potential interferences caused by the release of PFAS from the materials used for setup, the PFAS release was first checked to select the best type of material for connection tubes and columns.

A variable-speed peristaltic pump (BT100S-1) was used to pass deionized water through tubes made of Viton, silicone, and Tygon at a flow rate of 2.13×10^{-9} m^3/s. (0.128 mL/min) for one hour. Two sections of columns, made of glass and PMMA (polymethyl methacrylate), were left in separate containers filled with deionized

water for one hour. Additionally, deionized water was passed through the tubes connected to the column's inlet and outlet caps.

Samples were collected at time points 0 and 1 hour after contact. PFAS release was assessed for each sample using an HPLC-LM/MS instrument. No significant release of PFAS compounds was observed.

3.5 Adsorption of PFASs at Low Concentrations on the Different Materials in Column Test Setup

Since the primary goal of this work was to examine how PFASs behave at low concentrations, special care was taken to assess the possible background contamination or unintentional adsorption of the selected material for the setup. At this step, working with low concentration solutions enabled us to detect even small adsorption or release effects from the setup materials, which might have gone unnoticed at higher concentrations. This was accomplished by utilizing a peristaltic pump to circulate single solutions of PFBS, PFOA, and PFOS through the system at a constant flow rate of 1.67×10^{-8} m^3/s (1 mL/min), with a nominal concentration of 0.1 µg/L (100 ng/L). Since the batch tests for these compounds were performed in the glass bottles, a glass column was selected. Tygon (ID=0.89 mm) and PTFE parts for the caps were used for connections. At first, just the Tygon inlet tubing was attached, and samples were taken at 2.5, 5, 7.5, and 10-minute intervals, which corresponded to the solution's residence time inside the tubing. After that, the PTFE inlet cap was attached to the tubing, and to assess any further adsorption by the cap, the same sampling intervals were carried out. The entire arrangement was completed by connecting the outlet cap and the glass column. At the same time intervals, a final sampling round was conducted. All collected samples were analyzed using the HPLC-LC/MS method. Figure 13 depicts the configuration used for assessment of PFOA adsorption on the connection tubes and caps.

Figure 13. Configuration used for PFOA adsorption test

Table 16. Adsorption test of PFBS, PFOS, and PFOA on the setup materials (Concentration is expressed in ng/L)

Time (min)	Glass Column			Tygon Tubes			PTFE Cap		
	PFBS	PFOA	PFOS	PFBS	PFOA	PFOS	PFBS	PFOA	PFOS
0	118.2	129.8	111.2	122.6	129.8	111.2	118.2	129.8	111.2
2.5	134.7	192.6	80.3	126.0	189.4	81.2	124.8	190.2	67.2
5	133.3	188.3	91.0	128.4	181.7	91.9	131.3	212.3	77.2
7.5	141.6	170.6	110.6	119.0	174.2	108.5	117.9	187.9	83.3
10	137.3	167.9	102.0	124.0	170.3	92.3	132.9	171.6	95.9
Control (C0)	129.8	118.2	111.2	122.6	129.8	111.2	118.2	129.8	111.2

The concentration of PFBS, PFOS, and PFOA in ng/L, at different sampling intervals for different sections of the setup are reported in Table 16. For the PFBS, there is not a significant release or adsorption on Tygon tubes or caps compared to the control concertation. On the other hand, for PFOA the detected concentrations at these three different sections are higher than the control concentration, which represents a possible release of PFOA from these materials. For the PFOS the concentration is decreasing over time, showing its adsorption on the materials in the setup.

3.6 Column Test

In this study, a stepwise experimental approach was designed to systematically assess the movement, adsorption, and potential retardation of per- and polyfluoroalkyl substances (PFASs) under conditions that reflect both controlled laboratory settings and realistic environmental scenarios. At first, the work focused on understanding PFAS transport behavior in a non-reactive porous medium by conducting column transport tests using a column packed with only washed silica sand. These experiments were performed for individual PFAS compounds at a nominal concentration of 0.1 µg/L (100 ng/L). It has two main benefits. First, because of saturation effects or detection resolution constraints, it makes it possible to identify even very small amounts of adsorption, retardation, or loss in the system that could otherwise go unnoticed at greater concentrations. Furthermore, it can be safely assumed that no unexpected adsorption or interaction would occur within the sand matrix itself at higher concentrations if minimal adsorption or retardation is seen under these strict low-concentration conditions, especially in a non-reactive porous medium like sand.

This stage is necessary to guarantee that any retention or removal that is seen in later studies utilizing adsorptive materials—like granular activated carbon (GAC)—can be exclusively ascribed to the adsorbent and not the transport medium or other system elements.

Following these initial transport tests, the study advanced to conditions that more closely resemble real-world water contamination scenarios. In environmental waters such as groundwater, surface water, drinking water sources, and contaminated sites, PFASs rarely found as isolated compounds; rather, they are typically present as complex mixtures (Domingo & Nadal, 2019). Therefore, the adsorption performance

of granular activated carbon (GAC) was evaluated using a mixture of selected PFASs at a nominal concentration of 10 µg/L. This concentration was chosen to ensure that the adsorption behavior could be effectively monitored within a practical experimental timeframe and under conditions where analytical detection remains robust. A 5×10^{-6} kg (500 mg) dose of GAC was used as the adsorbent in the adsorption and transport test of PFAS on GAC. This amount was selected based on preliminary trials conducted with various GAC concentrations (20 mg, 40 mg, 100 mg, 200 mg, 600 mg, and 1 g). Although higher and lower dosages were tested, 500 mg was determined to be the most suitable considering experimental constraints such as solution volume, material availability, and the overall time frame.

At last step of this study a single PFBA transport test in sand with 500 mg GAC column was done. In industrial manufacturing there is a shift away from long-chain PFAS like PFOA and PFOS toward short-chain alternatives such as PFBA and PFBS. While this shift was intended to reduce bioaccumulation, it presents a new problem for water treatment. These short-chain compounds are known to be less effectively removed by GAC. Consequently, a GAC system initially designed to treat PFOA and PFOS may become progressively less effective as the influent PFAS profile evolves to include a greater proportion of these harder-to-treat short-chain replacements. (Li et al., 2023). To supplement the combination studies and further explore the unique behavior of short-chain PFASs an individual column transport test was conducted using perfluorobutanoic acid (PFBA) at a nominal concentration of 10 µg/L. Under controlled settings, the test was carried out to assess both transit and possible retention utilizing a column filled with sand and a specific layer of GAC. This method made it possible to directly compare the transport and adsorption characteristics of short-chain PFASs when evaluated individually and when they are present in a mixture in competition with other PFASs.

3.6.1 Column Design and Packing Configuration in PFAS Transport Experiments

Flow Rate Control and Tubing Time Measurement

It was crucial to calibrate the pump to achieve a consistent flow rate of 1.67×10^{-8} m^3/s (1mL/min). The calibration process began by starting the pump until a drop appeared at the end of the inlet tube. Once the drop was visible, the pump was temporarily stopped, and the exit point of the inlet tube was placed into a graduated cylinder. The pump and a stopwatch were then started simultaneously. Over a set period of time, the pump speed was adjusted incrementally to ensure the flow rate aligned with the target rate of 1 mL/min equal to the Darcy velocity of 7.78×10^{-4} (m/s). By monitoring the amount of liquid collected in the cylinder, adjustments were made to the pump speed until the desired flow rate was achieved. This calibration step ensured the accuracy and consistency of fluid flow throughout the experiment. To account for and eliminate any retardation or delay caused by the tubing itself, the inlet and outlet times correspond to the residence time within the connection tubing, including Tygon tubes with an inner diameter of 0.89 mm and the PTFE tubes in the caps and connections to the collector and spectrophotometer used in the tracer test—were measured. The inlet tube was connected to a peristaltic pump, with the entrance of the tube placed in a beaker filled with deionized water. The other end of the inlet tube was attached to the entrance cap of the glass column. To initiate the test, the pump was activated, and a timer was started simultaneously to measure the time required for the first drop of water to reach the entrance of the column. This process was repeated for each tubing connection.

Column Packing

For all the tests, a glass column with 1.65×10^{-2} m inner diameter was used. To prevent air bubbles— a significant issue in saturated column tests, the deionized water was added to the washed sand and were degasified under the vacuum treatment to remove any trapped air, ensuring that the packing material was fully saturated and free of bubbles. For the *individual PFASs transport test in only-sand column*, the actual packing of the column began with the careful addition of a 1 cm layer of Dorsilit 5G, coarse grain at the bottom of the column. This layer served as a filtration medium, helping to prevent smaller particles entering the tubing part and a layer for

flow homogenization on the cross section. Following this, as the deionized water was slowly pumped into the column, 34 gr of D8, corresponding to 11 cm was added gradually, allowing for adequate saturation after each addition. This slow process helped to ensure that the material settled uniformly without creating voids. Once the 11 cm of packed material was in place, another 1 cm layer of DG5 coarse grain was added to the top of the column. This final layer served to stabilize the packing while avoiding clogging and further preventing the escape of fine particles. The column was then carefully capped to avoid any disturbance to the packed layers before proceeding to the next phases of the experiment.

For the *adsorption transport tests of the mixture of PFASs and PFBA on the GAC*, a glass column 1.65 cm inner diameter was utilized. To avoid air bubbles, which can have a major impact on the results, all materials were properly degasified. Before the column was packed, deionized water was combined with 500 mg of granular activated carbon (GAC) and 6.8 g of D8 sand in separate beakers. Then all materials, along with the deionized water and PFAS solutions, were degassed using vacuum treatment to remove dissolved gases and trapped air.
The column packing process began with the careful addition of a 0.5 cm layer of coarse Dorsilit 5G at the bottom of the column, serving as a filtration medium and supporting the packed structure. While deionized water was slowly pumped into the column to allow full saturation, 3.4 g of D8 sand, corresponding to a 0.75 cm layer, was gradually added in small portions, ensuring adequate wetting and compaction at each step. Once the bottom sand layer was in place, the pump was temporarily stopped to allow for the addition of the GAC layer because GAC has lower density compared to sand and tends to float in water if the pump remains running during its addition. 500 mg of pre-washed and degassed GAC, corresponding to approximately 0.5 cm in height, was gently introduced into the column. After the GAC layer was in place, the remaining 0.75 cm of D8 sand was gradually added on top, while reactivating the pump to maintain water saturation and minimizing air entrapment. Finally, a 0.5 cm layer of Dorsilit 5G was added at the top of the column to stabilize the packing.

The column was then carefully sealed with caps to prevent any disturbance to the packed structure, ensuring uniformity before proceeding with the transport experiments.

3.7 Tracer Test

Tracer tests help characterize the flow dynamics within the porous medium, providing insights into how the water and solutes move through the system. By identifying potential issues such as preferential flow paths or dead zones, tracer tests ensure that the transport parameters calculated during column tests accurately reflect real fluid behavior. These preliminary tests help in determining hydrodynamic dispersion, retention time, and channeling effects.

In this study, before performing any column transport test with PFASs solutions, the tracer tests were carried out for the same column and with same configuration and flowrate explained in the section 3.6.1 to assess wisely the flow dynamics in the columns and estimate the porosity, Dispersivity and retention time of different materials in the column in the saturated condition.

A potassium bromide (KBr; CAS No. 7758-02-3, Chem Lab, Belgium) solution was prepared in deionized water at concentrations of 0.005 mol/L (5 mM) and 0.0025 mol/L (2.5 mM) for use as a conservative tracer in the column transport tests for the only-sand and sand plus GAC configurations, respectively. Prior to tracer injection, the columns were thoroughly flushed with deionized water to remove colloidal particles, and potential impurities, ensuring uniform flow conditions. The tracer solution was then injected into the columns using a peristaltic pump set at a constant flow rate of 1 mL/min.

Effluent samples were monitored every 30 seconds for absorbance at a wavelength of 198.5 nm using a UV-Vis spectrophotometer (SPECORD S 600, Analytik Jena GmbH, Germany) equipped with a quartz flow cell with 5 mm path length, directly connected to the column outlet. Additionally, the presence of colloids or suspended particles was assessed by measuring absorbance at 400 nm and 500 nm. Figure 14 shows the setup used for tracer test for only sand columns. The same configuration was used for tracer test for sand with GAC columns.

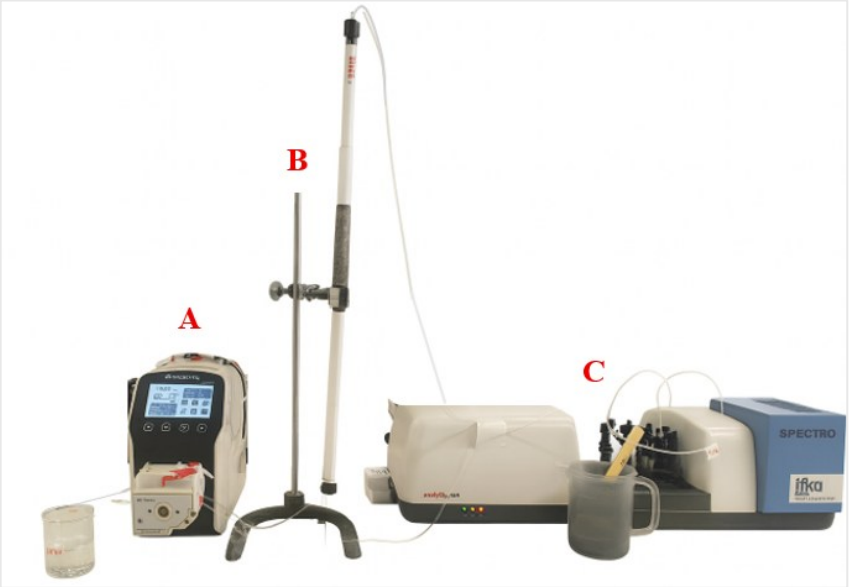

Figure 14. Tracer test setup for only sand column, A: peristaltic pump, B: column, C: spectrophotometer

To better understand the porosity and flow path of the columns containing GAC, two same tracer tests with KBr 0.0025 mol/L (2.5 mM) were performed with the 3cm column packed with only crushed GAC which was used in transport tests and 3 cm column packed with only uncrushed GAC. 2 gr of crushed GAC and 2 gr of uncrushed original GAC were soaked in deionized water separately for 1:30 hours, then gone under the vacuum treatment to remove all the air bubbles. The packing starts with 0.5 cm layer of coarse Dorsilit 5G at the bottom of the column, serving as a filtration medium and supporting the packed structure, while the water pumped in slowly, 2 cm of crushed GAC gradually added and the column was tapped to remove the air, then finally a 0.5 cm layer of Dorsilit 5G was added at the top of the column to stabilize the packing. The same packing was done with original GAC. Before injection water and tracer solution were degasified. After the packing was finished, the column was flushed with deionized water for half an hour till all the particles were removed and the absorbance of particles and colloids was close to zero. Then, the tracer was injected at a constant flowrate of 1 ml/min. This approach enabled accurate monitoring of the tracer breakthrough curves, which were subsequently used to calculate the pore volume time and assess hydrodynamic behavior. The tracer tests

results were further analyzed and modeled through the inverse solution, solute transport - single porosity van Genuchten-Mualem model in equilibrium mode using Hydrus 1-D software to estimate key transport parameters, including water content and Dispersivity of the materials used in packing. Then using the obtained parameters, the PFASs transport test results were modeled to estimate the PFASs reaction coefficient; Kd (distribution coefficient) and retardation factor.

3.8 Individual PFASs Transport Tests_Only Sand Column

After performing the tracer test and checking the PFASs release and adsorption of the material, individual PFASs column transport tests were conducted for all the 4 selected PFASs with a nominal concentration of 0.1 µg/L (100 ng/L), using only-sand column described in section 3.6.1. Considering the obtained pore volume time equal to 10 minutes from the tracer tests, the PFASs solutions were injected 10 pore volume times (100 minutes). During this period, from the effluent, 6 samples were collected every 0.5 PV (5 minutes), followed by 7 samples every PV (10 minutes). Subsequently, deionized water was injected for another 10 pore volume times, and 8 samples were collected every 0.5 PV, followed by 6 samplings every PV. Additionally, every PV, 1 sample was collected from the bypass (overall 20 samples for bypass). The concentration of the influent was controlled before injection. The samples were analyzed with HPLC-LM/MS method. The breakthrough curves obtained from this experiment are shown in Figure 20.

3.9 PFASs Competitive Adsorption Transport Test _Sand with GAC Column

As explained in section 3.6, a column transport test was carried out to look into the competitive adsorption behavior of the four selected PFASs onto GAC. This test was done to simulate more realistic settings where PFASs usually occur as mixes in aquatic environments.

A solution of a mixture of 4 compounds was prepared with a nominal concentration of 10 µg/L. After flushing the column with deionized water overnight, a sample from the effluent was analyzed to control for the possible release of PFASs before

injection. The mixture solution was injected for 7 days (173 hours), and then the deionized water was injected to flush the column. Samples from the effluent were collected every hour and analyzed using HPLC-LM/MS method. The concentration of the influent was controlled every day. Thanks to the fraction collector (model Teledyne ISCO Foxy Jr., USA) the test could be performed overnight and during weekends and holidays. The composition and configuration of the column is described in section 3.6.1.

3.10 Adsorption Transport Test of PFBA - Sand with GAC Column

As was discussed in section 3.6; to investigate the adsorption of PFBA on the GAC, a column transport test was performed with the solution of PFBA with a nominal concentration of 10 µg/L. All materials, including sand, GAC, deionized water, and the mixture solution, were degassed under vacuum before injection. After flushing the column with deionized water overnight, a sample from the effluent was analyzed to control for the possible release of PFASs before injection. The solution was injected for 16 days (388 hours), and then the deionized water was injected to flush the column. Samples from the effluent were collected every hour and analyzed using HPLC-LM/MS method. The concentration of the influent was controlled every day. The test was performed overnights and during weekends and holidays using the fraction collector. The composition and configuration of the column is described in section 3.6.1.

Figure 15 illustrates the setup configuration used for competitive PFASs transport test and PFBA transport test.

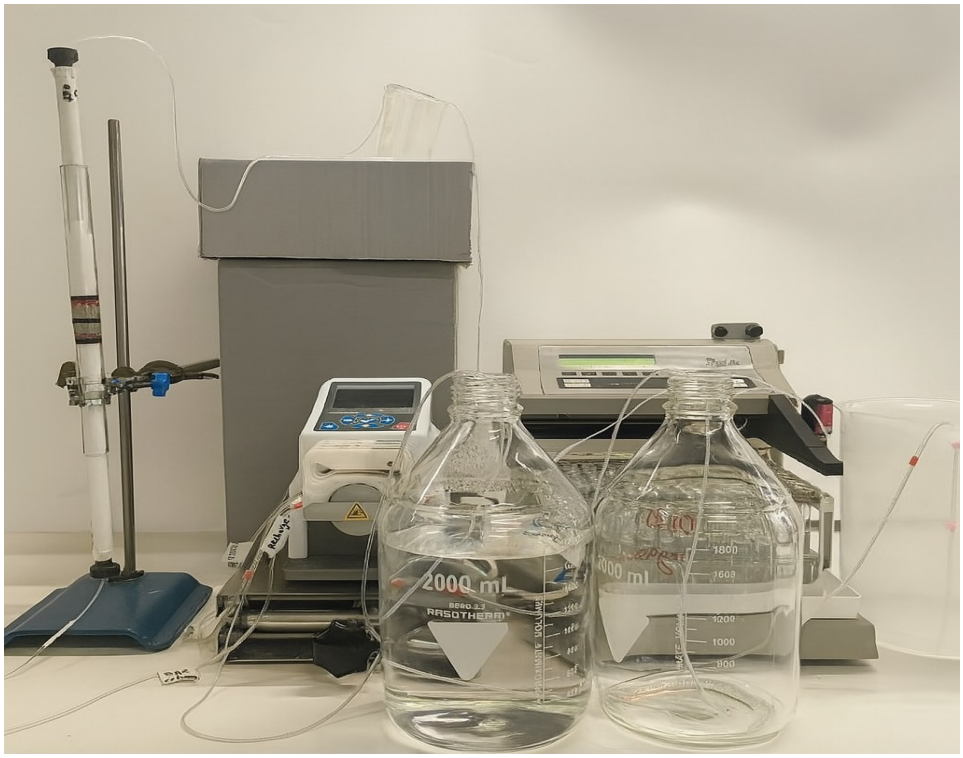

Figure 15. PFAS transport test-setup configuration

Chapter 4

4. Results

4.1 Breakthrough Curves-Tracer Test

The breakthrough curves obtained from the tracer tests for columns packed with only sand, and sand with GAC are illustrated in Figure 16 and Figure 17, respectively.

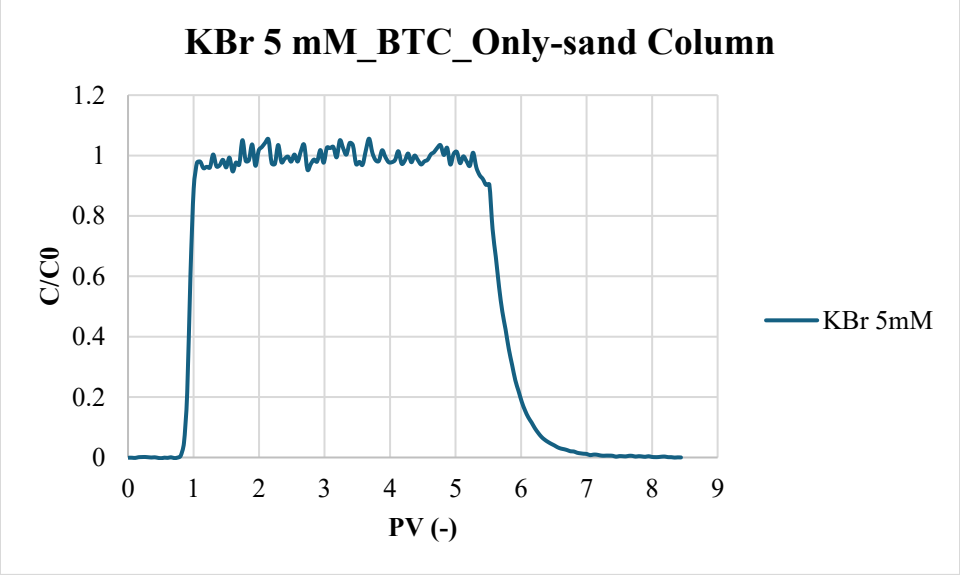

Figure 16. Breakthrough curve of KBr 5 mM for the only sand column

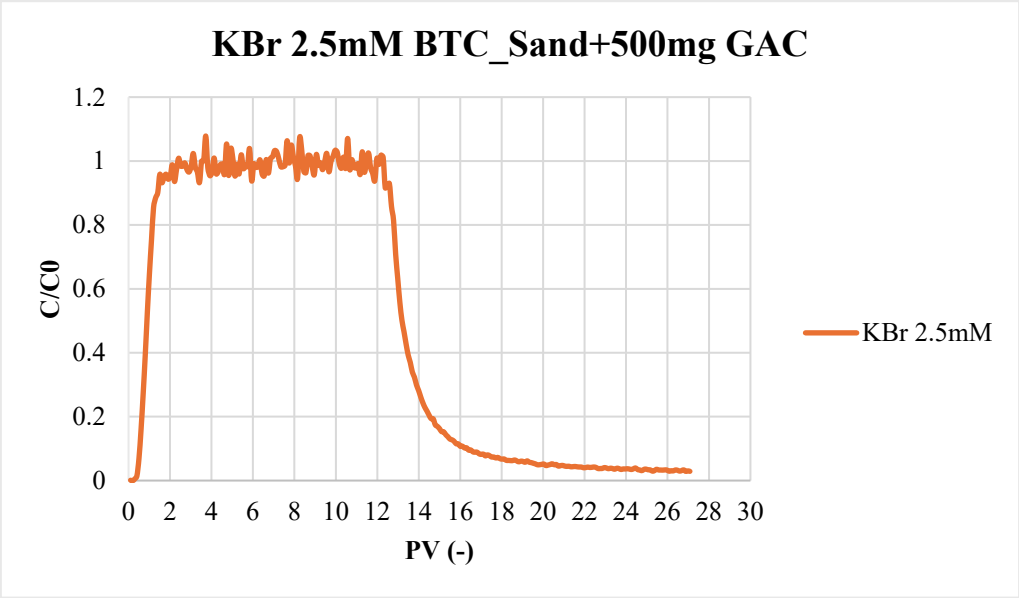

Figure 17. Breakthrough curve of KBr 2.5 mM for sand with GAC column

The pore volume time for the column packed with only sand is 10 minutes and for column packed with sand plus GAC is 5 minutes.

The breakthrough curves obtained from the tracer tests for columns packed with only crushed GAC, and only original GAC are illustrated in Figure 18 and Figure 19, respectively.

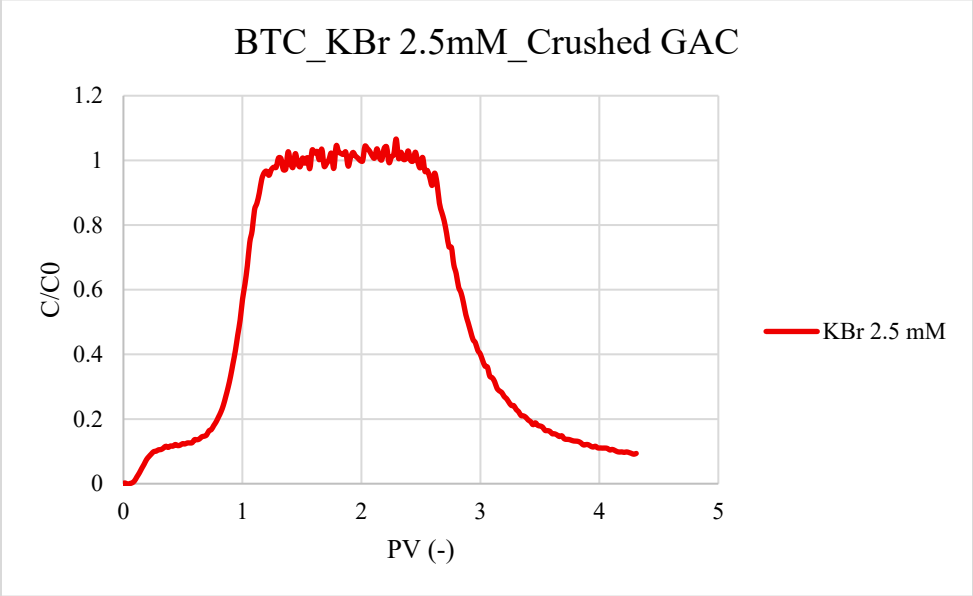

Figure 18. Breakthrough curve of KBr 2.5 mM for crushed GAC column

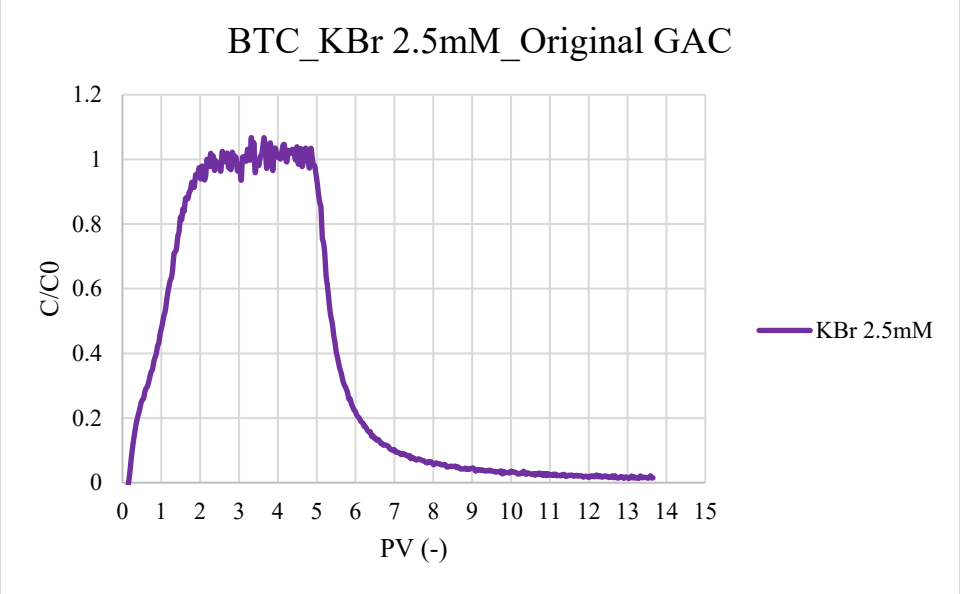

Figure 19. Breakthrough curve of KBr 2.5 mM for uncrushed original GAC column

The pore volume time for the column packed with crushed GAC is 25 minutes and for column packed with original GAC is 15 minutes. The early breakthrough seen in the first parts of the curves reflects the significant influence of macroporosity, which

makes a fast tracer movement due to advective transport. Higher pore volume time for the crushed GAC column indicates a higher effective porosity in the crushed GAC bed due to denser packing and greater internal pore volume.

4.2 Hydrus 1-D Modeling Results for Individual PFASs Transport Test- Only-Sand Column

As discussed in section 3.7, using the experimental data obtained from the tracer tests and column transport tests performed for the individual PFASs in only-sand media, the water content, Dispersivity were estimated for this column and , Kd, retardation factor (R), were estimated for the Individual PFASs transport test, Table 17. The results show clear differences in the mobility and sorption behavior of these compounds. PFBS exhibited the lowest sorption, with a Kd of 0.31×10^{-4} m^3/kg and a retardation factor (R) of 1.006, indicating it moved at the same rate as water, consistent with its short-chain structure. In contrast, PFOS showed the strongest interaction with the sand, with a Kd of 2.2×10^{-4} m^3/kg and an R of 1.048, reflecting significant retardation due to its long-chain sulfonate structure. PFOA and PFBA demonstrated moderate sorption, with retardation factors of 1.025 and 1.035 respectively.

Table 17. Estimated hydraulic and reaction parameters by Hydrus 1-D for only-sand column transport tests

Comp.	Water Content	Dispersivity (m)	Pore-water Velocity (m/s)	Dispersion (m^2/s)	Kd (m^3/kg)	R
PFBA	0.302	1.2×10^{-4}	2.58×10^{-4}	3.09×10^{-8}	1.84×10^{-4}	1.035
PFBS	0.319	1.5×10^{-4}	2.44×10^{-4}	3.66×10^{-8}	0.31×10^{-4}	1.006
PFOA	0.328	2.6×10^{-4}	2.37×10^{-4}	6.16×10^{-8}	1.21×10^{-4}	1.025
PFOS	0.341	1.6×10^{-4}	2.28×10^{-4}	3.65×10^{-8}	2.2×10^{-4}	1.048

The water content and Dispersivity of the crushed GAC and original GAC is reported in Table 18. To estimate these parameters, the Kd was considered a reaction parameter for the tracer. Otherwise, the data could not be fitted with the model (R^2<0.3).

Table 18. Estimated hydraulic parameters by Hydrus 1-D for crushed GAC column

Column	WCS	Pore water Velocity (m/s)	Disp (m)	Kd (m^3/kg)
Original GAC	0.64	1.21×10^{-4}	7.9×10^{-3}	3.9×10^{-3}
Crushed GAC	0.5	1.56×10^{-4}	6×10^{-4}	6.55×10^{-3}

4.3 Results of Individual PFASs Transport Tests_Only Sand Column

The breakthrough curves obtained from each individual PFASs column transport test, with the media of only sand, are compared and shown in Figure 20. The pore volume time is 10 minutes. The mass balance and initial concentration (C0) for these 4 compounds are reported in Table 19. As observed, the concentration ratio (C/C_0) for PFBS, PFOA, and PFBA increases rapidly at the beginning and reaches approximately 0.5 after about 1 pore volume (PV). After 2 PV, the ratio approaches unity and remains stable up to around 10 PV during the PFAS compound injection phase. Following this, the injection of deionized water causes the concentrations to drop sharply to zero, indicating complete flushing and removal of these compounds from the column after 2 PV. This behavior suggests that there is no significant adsorption or chemical interaction between these three compounds and the sand matrix. The breakthrough curves closely resemble those of a conservative tracer, indicating that PFBS, PFOA, and PFBA behave conservatively in the sand column. This is aligned with the obtained retardation factor for these compounds. However,

PFOS exhibits different behaviors. Its concentration does not reach unity and shows a slightly delayed breakthrough compared to the others. It could be due to possible adsorption on the materials or setup. Moreover, the presence of tailing at the end of the test indicates its stronger interaction. As anticipated for silica, a negatively charged, low-adsorbing media, all PFASs demonstrated comparatively quick breakthrough with little retention. As expected for short chain PFASs, given their poor hydrophobicity compared to the longer chains and sparse interactions with the solid matrix, PFBA and PFBS eluted quickly. The highest retention was shown by PFOS. This tendency, especially for longer-chain sulfonates like PFOS, is ascribed to interfacial partitioning processes or weak hydrophobic contacts rather than adsorption on silica sand. The obtained mass balance, Table 19, proves the less adsorption of short chains and slight adsorption of long chains.

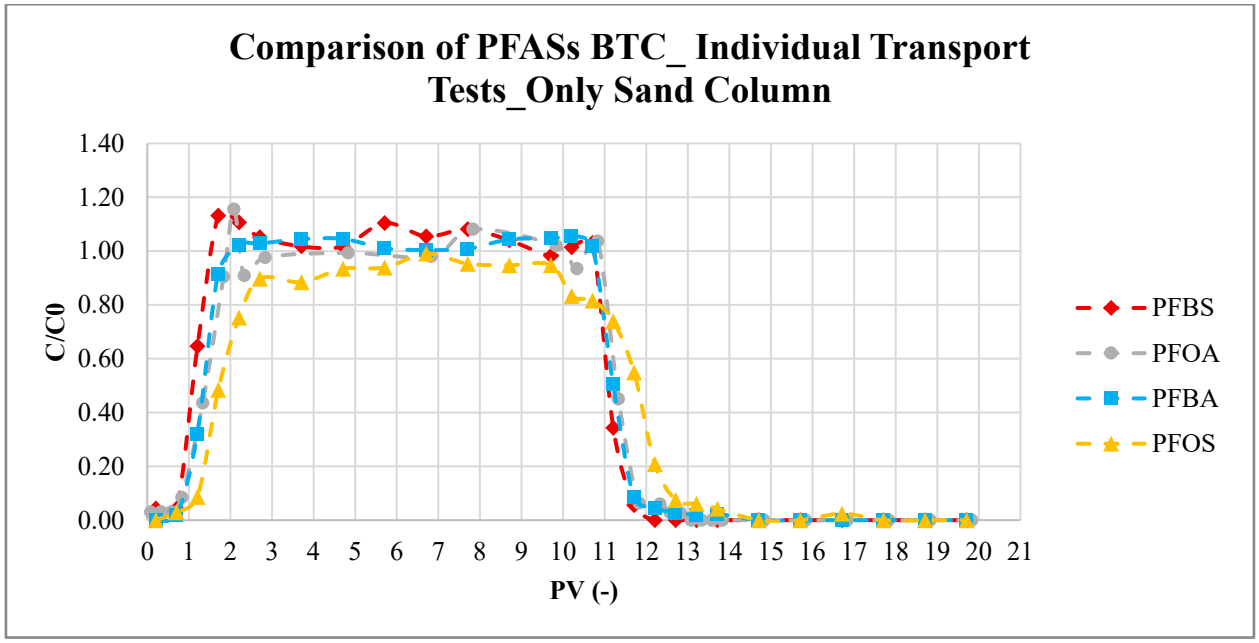

Figure 20. Comparison of breakthrough curves obtained from individual PFASs transport tests- only sand column

Table 19. Mass balance and initial concentration of individual PFASs transport test-only sand column

Compound	Concentration of the Control (ng/L)	Percentage of Mass Balance(M/M0)
PFBA	157.26	102.43
PFBS	155.58	102.61
PFOA	170.68	97.71
PFOS	108.6	93.54

4.4 Results PFASs Competitive Transport Test _Sand with GAC Column

Figure 21 indicates the breakthrough curves of the transport test for PFASs competitive adsorption on GAC. The breakthrough curves' horizontal axis shows how many pore volumes (PV) have gone through the column. The injection phase is equivalent to roughly 2,076 pore volumes given a pore volume time of 5 minutes and a total injection period of 173 hours, almost 7 days. The length of the carbon chain, the kind of functional group, and the molecular structure of each analyte are all intimately related to the sequence of breakthrough that was observed. With its relative effluent concentration (C/C_0) nearing unity, 0.8, PFBA showed the fastest breakthrough. Its short fluorocarbon chain and carboxylate functional group, which produce the weakest hydrophobic and electrostatic interactions with the GAC

surface, are responsible for this behavior. Furthermore, the saturation of accessible adsorption sites was probably exacerbated by the much higher observed influent concentration for PFBA (19.22 µg/l). After roughly 200–300 pore volumes, PFBS breakthrough started. Because the sulfonate functional group has a higher adsorption affinity than the carboxylate group of PFBA, it was retained more than PFBA; nevertheless, because of its short chain, it was retained much less than the long-chain compounds.

Conversely, PFOA exhibits strong retention, with breakthrough starting after a notable delay of roughly 600–700 pore volumes. Over an extended injection period, the long C8 chain improves hydrophobic interactions with the GAC, resulting in efficient removal. Even after injecting more than 2,000 pore volumes, PFOS continued to exhibit the highest affinity for the GAC with no discernible breakthrough. The highest adsorptive interactions are produced by a long C8 chain and a sulfonate functional group, which leads to almost total elimination during the injection phase.

One important finding from Figure 21 is that, at the end of the injection phase, none of the compounds had achieved full saturation ($C/C_0 = 1$). It should be noted that the concentration of the influent decreased during the experiment. In general, as the influent concentration increases, the breakthrough time decreases. This is because a higher concentration leads to a quicker saturation of the adsorbent material (Chowdhury & Saha, 2012) while lower influent concentrations favor adsorption and deposition, delaying breakthrough and producing more gradual breakthrough curves (Wei, Shao, Du, & Horton, 2014). A decreasing influent concentration means that the amount of adsorbate introduced into the system lessens as time progresses (Abdulhusain & Abd Ali, 2023) . This reduction affects the saturation rate of the adsorbent material and, consequently, the breakthrough curve. When the adsorbent is subjected to a lesser challenge over time, this might result in an apparent breakthrough delay and an underestimation of the adsorption capacity. The breakthrough point, which is the time at which the effluent concentration starts to increase, will be delayed because the adsorbent takes longer to become saturated and the maximum concentration reached at breakthrough may be lower compared to a scenario with a constant or increasing influent concentration. In a competitive transport test, a decreasing influent concentration over time will generally result in a delayed and less pronounced breakthrough curve for the compounds even with higher

affinity, altering the dynamics of competition for adsorption sites. As the concentration of the influent decreases, there are fewer molecules competing for the available adsorption sites. This reduced competition can enhance the adsorption of other substances present, even with weaker affinity for the adsorbent (Gu, Mehlhorn, Liang, & McCarthy, 1996). This phenomenon is in line with the breakthrough behavior seen in the current study; even though long-chain compounds like PFOA and PFOS have a higher affinity for GAC, their influent concentrations were significantly lower in the later stages of injection compared to other two compounds over time. Consequently, their C/C_0 values stayed below unity (about 0.6 for PFOA and 0.78 for PFOS), which was caused by inadequate mass loading and a reduced driving force rather than total adsorption or lack of desorption. In the meantime, PFBA and PFBS, which first appeared when concentrations were still quite high, attained greater C/C_0 values (~0.8).

Moreover, the injection phase's 173 hours were not enough to completely deplete the GAC bed's capacity for PFBS, PFOA, and particularly PFOS. Also it should be mentioned that in this experiment, performing an experiment with time and material feasibility consideration, the length of the column and amount of adsorbent may not well represent a complete porous media and since this small layer of GAC does not provide enough residence time for pollutants to well contribute to the adsorption on the GAC, the occurrence of fast breakthroughs is observed. Increasing the amount of GAC and its surface area should be considered for future studies. The fraction of injected mass recovered in the effluent (M/M_0) varied between 38.22 % and 47.09% for each of the four chemicals, according to the mass balance data in Table 20. It can represent possible adsorption of PFASs along the setup. Selecting rapid small-scale column test (RSSCT) and materials with less adsorption of PFASs like stainless steel and shortening the connections as much as possible would constrain the possible release and adsorption of PFASs.

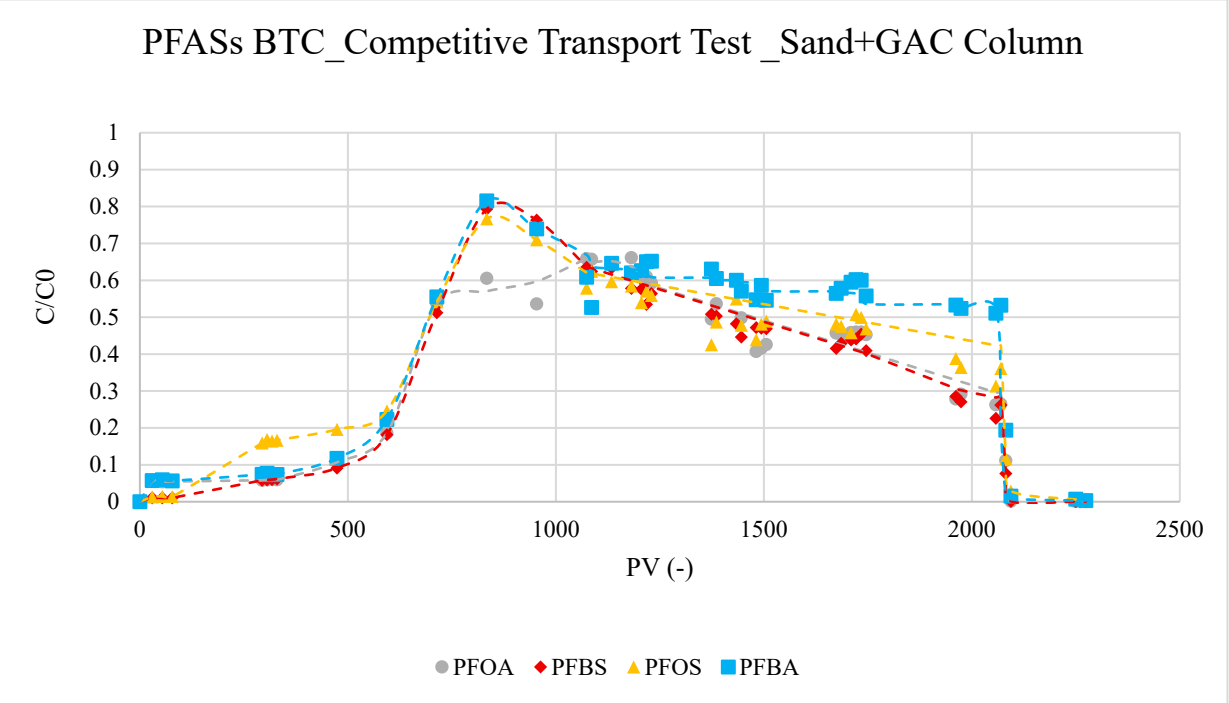

Figure 21. Comparison of the breakthrough curves of PFASs competitive adsorption transport test- sand with GAC column

Table 20. Mass balance from PFASs competitive adsorption transport test- sand with GAC column

Compound	Concentration of the Control (µg/l)	Percentage of Mass Balance(M/M0)
PFBA	19.22	47.09
PFBS	11.31	39.31
PFOA	9.26	38.88
PFOS	7.07	42.99

4.5 Results of PFBA Transport Test – Sand with GAC Column

The breakthrough curve for the adsorption of Perfluorobutanoic acid (PFBA) onto GAC is illustrated in Figure 22. The horizontal axis shows how many pore volumes (PV) have gone through the column. The injection phase is equivalent to roughly 4656 pore volumes given a pore volume time of 5 minutes and a total injection period of 388 hours, 16 days. The y-axis represents the normalized effluent concentration (C/C0), which is the ratio of the effluent PFBA concentration (C) to the influent concentration (C0).

In the initial stage of the experiment, the normalized effluent concentration remains near zero (C/C0≈0). This indicates that the GAC adsorbent is fresh and has sufficient available active sites for PFBA, resulting in nearly complete removal from the aqueous phase.

After 1000 to 2500 PV there is a steep increase in the C/C0 ratio, signifying the progressive saturation of the GAC bed. The midpoint of the mass transfer zone (C/C0

=0.5) is reached at approximately 1400 PV. The shape and slope of this front are dictated by mass transfer kinetics and dispersion phenomena within the column.

Following the sharp breakthrough, the curve begins to plateau as it approaches unity. In this phase, the GAC bed is considered exhausted or saturated with PFBA. The adsorbent has lost most of its capacity, and the effluent concentration approaches the influent concentration (C/C0→1). The observed fluctuations in this region, hovering between C/C0 values of 0.8 and 0.95, may be attributed to experimental variability or complex, slow-adsorption kinetics that prevent the immediate attainment of full stoichiometric saturation (C/C0=1.0) and it needs the experiment be continued for longer time. Increasing the residence time and the adsorbent concentration would increase the adsorption interactions. Moreover, performing transport test with modified GAC or anion exchange resins can be considered for further assessment in removing short chain PFASs as showed better performance in removing short chain PFASs (Riegel, Haist-Gulde, & Sacher, 2023) (McCleaf et al., 2017).

As shown in Figure 23, comparing the breakthrough curves of single PFBA transport test and the competitive PFASs adsorption test, in the case of single-component adsorption, the initial breakthrough occurs relatively late; concentration increases smoothly and steadily, eventually approaching unity. In contrast to competitive adsorption, the occurrence of a roll-up peak is not expected under single transport conditions. In the competitive transport test, the GAC's capacity for PFBA is diminished because other substances have a higher affinity for the adsorbent, occupy the active sites that would otherwise be available to PFBA while without any competitors, the GAC can effectively remove PFBA for a significant amount of time before it becomes fully saturated. In the competitive test C/C0= 0.5 is obtained at PV 600 while it is obtained at PV 1400 in single test.

It implies that in a real-world scenario where water contains a mixture of contaminants, a GAC filter would need to be replaced far more frequently to ensure effective removal of weakly adsorbing compounds like PFBA.

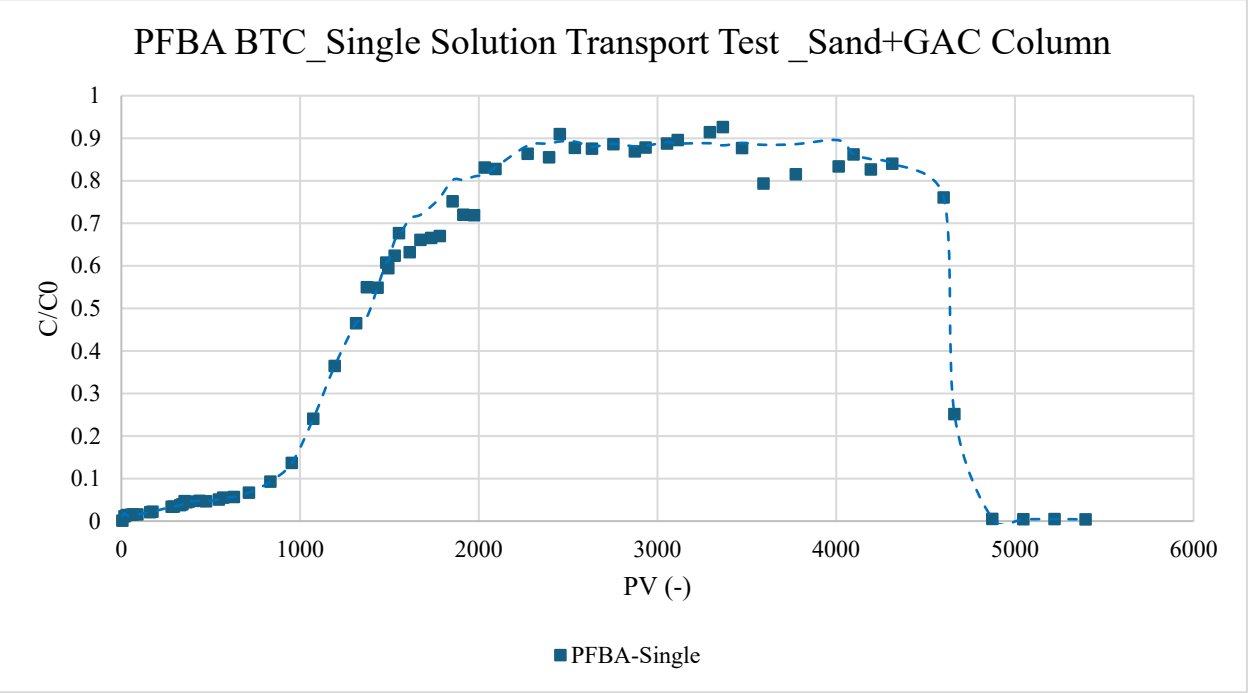

Figure 22. PFBA breakthrough from transport test- sand with GAC column

The mass balance for the PFBA transport test is reported in the Table 21. According to mass balance analysis, only 61.5% of the injected PFBA was recovered at the column output, indicating a partial retention inside the GAC bed. This insufficient recovery suggests slow desorption or kinetically limited adsorption processes that were not fully captured during the study time.

Table 21. Mass balance from PFBA transport test- sand with GAC column

Compound	Concentration of the Control (µg/l)	Percentage of Mass Balance (M/M0)
PFBA	30.23	61.49

Although the influent concentration for single and competitive tests were different, and the differences in initial influent concentrations can influence the actual mass loading on the GAC, just for comparing the sizing, a constant influent concentration was assumed and given the characteristics of the experimental setup and adsorbent, Table 22; the flow rate during the column test equals to $1.67 \times 10^{-8}\ m^3$, the GAC bed volume of $1.07 \times 10^{-6}\ m^3$, corresponding to a bed depth of 0.005 m and a GAC mass of 5×10^{-4} kg, the empty bed contact time (EBCT) for the layer of GAC was obtained 1.07 minutes.

The breakthrough point ($C/C_o = 0.5$) in the single-solute PFBA test was reached at 1400 pore volumes, corresponding to a treated volume of $7 \times 10^{-3}\ m^3$. While in the competitive adsorption test, breakthrough occurred at just 600 pore volumes, $3 \times 10^{-3}\ m^3$. To achieve the same treated volume under competitive conditions, the GAC bed would need to be scaled by a factor of 2.33, increasing the GAC mass to 1.165×10^{-3} kg and the bed depth to 0.0115 m.

Table 22. Characteristics of experiment setup and adsorbent

Column cross section (m^2)	Length of the GAC layer (m)	Flowrate (m^3/s)	GAC bed volume (m^3)	Pore volume time (min)
2.14×10^{-4}	0.005	1.67×10^{-8}	1.07×10^{-6}	5

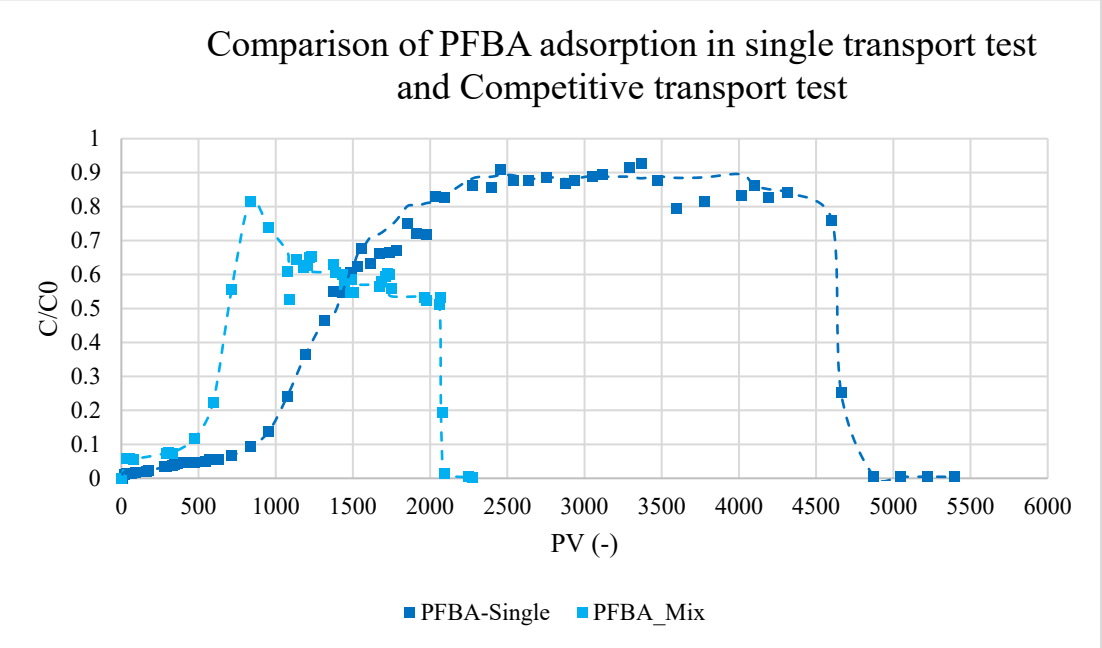

Figure 23. Comparison of PFBA adsorption on GAC in single and competitive transport tests

Chapter 5

5. Conclusion

The focused column experiment results in this research improved our knowledge about how PFAS move and adsorbed to granular activated carbon systems. The distinct breakthrough behaviors and sorption capacities confirm that PFAS remediation strategies require individual compound analysis. Each PFAS compound has a distinct molecular structure which determines its ability to bind with adsorbents and how easily it can be treated.

PFAS removal through GAC is effective but depends heavily on operational parameters including adsorbent dosage and influent concentration and flow rate. The treatment process benefits from lower flow rates and concentrations but operational limitations from system design and treatment capacity must be considered for practical applications. The adsorbent requires larger interaction sites together with longer contact duration to achieve the best removal results.

This research demonstrates that granular activated carbon (GAC) columns show different adsorption behaviors toward PFAS compounds based on their functional groups and carbon chain lengths. The research demonstrated that GAC adsorbs PFOA and PFOS better than PFBA and PFBS through its experimental observations. Zeng et al. (2020) confirms this pattern through their research that demonstrates long carbon chains in perfluorosulfonic acid (PFSA) and perfluorocarboxylic acid (PFCA) compounds produce both extended breakthrough times and improved adsorption properties in column systems (Zeng et al., 2020).

The only-sand column test provided valuable insights about PFAS movement under basic porous media conditions. The PFAS compounds experienced minimal delays in their breakthrough behavior when passing through the sand medium. The research shows that sand material lacks the ability to remove PFAS especially the short-chain mobile variants when PFAS saturation occurs which makes them behave like tracers. The research by Lyu et al. shows that adsorption at the air–water interface under unsaturated conditions produces major retardation in PFAS movement through sandy porous media but these conditions were not met in our investigation. This research demonstrates that PFAS retention was limited in saturated sand conditions, so GAC stands as the necessary advanced treatment material to effectively manage water source PFAS pollution (Lyu et al., 2018).

GAC remains a fundamental component of PFAS treatment, but additional innovations must be developed to handle new PFAS compounds while enhancing regeneration methods and extending the life span of adsorption media. The future research agenda should examine adsorbed PFAS stability over time while studying hybrid adsorbents and validating experimental results using pilot and full-scale systems. A combination of experimental rigor and engineering adaptability represents our only path to stay ahead of the continuous evolution of PFAS contamination threats.

Suggestions for Future Experiments

Multiple future research directions should focus on improving PFAS adsorption on GAC to develop better treatment methods through the following initiatives:

1. Extended breakthrough experiments: The GAC bed did not reach complete saturation during the testing period according to the study. Future investigations need to extend the injection time to achieve complete saturation of all target PFAS chemicals. The GAC's total adsorption capacity for each component would become more precise under competitive conditions with this extension. Moreover increasing the adsorbent dosage is a crucial factor to better assess the GAC capacity in removing PFASs.

2. Future research needs to investigate the effects of co-contaminants such as humic acids and inorganic ions and dissolved organic matter (DOM) on PFAS adsorption efficiency. Compounds create more complex real-world water matrices through their influence on breakthrough curves and their competition for GAC adsorption sites.

3. The current study maintained constant pH but a systematic investigation of competitive PFAS adsorption under different temperature and pH conditions would provide essential data for optimizing GAC performance in various environmental applications. The surface charge of GAC and PFAS speciation experience changes due to these elements. Moreover, the rate of breakthrough and adsorption efficiency changes based on different flow rates. This information would help optimize the empty bed contact time (EBCT) for various PFAS concentrations and combinations.

4. Future research should focus on developing and testing new adsorbent materials which are specifically designed to remove short-chain PFAS compounds because these substances are generally more challenging to remove in the real-world scenario where short chain PFASs outcompeted by long chains in adsorption on GAC as a common adsorbent.

References

Australian Drinking Water Guidelines 6, Version 3.9, (2011).

(EEA), E. E. A. (2024). PFAS pollution in European waters. Retrieved from https://www.eea.europa.eu/en/analysis/publications/pfas-pollution-in-european-waters

(EPA), U. S. E. P. A. (2021). Multi-Industry Per- and Polyfluoroalkyl Substances (PFAS) Study – 2021 Preliminary Report. Retrieved from https://www.epa.gov/system/files/documents/2021-09/multi-industry-pfas-study_preliminary-2021-report_508_2021.09.08.pdf

(ITRC), I. T. R. C. (2023). PFAS Technical and Regulatory Guidance Document

Retrieved from https://itrcweb.org/pfas-guidance/

Abdulhusain, N. A., & Abd Ali, Z. T. (2023). Green approach for fabrication of sand-bimetallic (Fe/Pb) nanocomposite as reactive material for remediation of contaminated groundwater using permeable reactive barrier. *Alexandria Engineering Journal, 72*, 511-530.

Agency, U. S. E. P. (2025). Per- and Polyfluoroalkyl Substances (PFAS) under the Safe Drinking Water Act. Retrieved from https://www.epa.gov/sdwa/and-polyfluoroalkyl-substances-pfas. from EPA https://www.epa.gov/sdwa/and-polyfluoroalkyl-substances-pfas

Appleman, T. D., Dickenson, E. R., Bellona, C., & Higgins, C. P. (2013). Nanofiltration and granular activated carbon treatment of perfluoroalkyl acids. *Journal of hazardous materials, 260*, 740-746.

ATSDR. (2021). Toxicological profile for perfluoroalkyls. In: Agency for Toxic Substances and Disease Registry editor. Atlanta, GA.

Barbero, I. (2024). *Adsorption of PFAS on activated carbon*. (Master). Polytechnic University of Turin,

Behnami, A., Pourakbar, M., Ayyar, A. S.-R., Lee, J.-W., Gagnon, G., & Benis, K. Z. (2024). Treatment of aqueous per-and poly-fluoroalkyl substances: a review of biochar adsorbent preparation methods. *Chemosphere*, 142088.

Belkouteb, N., Franke, V., McCleaf, P., Köhler, S., & Ahrens, L. (2020). Removal of per-and polyfluoroalkyl substances (PFASs) in a full-scale drinking water treatment plant: Long-term performance of granular activated carbon (GAC) and influence of flow-rate. *Water research, 182*, 115913.

Bhhatarai, B., & Gramatica, P. (2011). Prediction of aqueous solubility, vapor pressure and critical micelle concentration for aquatic partitioning of

perfluorinated chemicals. *Environmental Science & Technology, 45*(19), 8120-8128.

Buck, R. C., Franklin, J., Berger, U., Conder, J. M., Cousins, I. T., De Voogt, P., . . . van Leeuwen, S. P. (2011). Perfluoroalkyl and polyfluoroalkyl substances in the environment: terminology, classification, and origins. *Integrated environmental assessment and management, 7*(4), 513-541.

Canada, H. (2024). Objective for Canadian drinking water quality per- and polyfluoroalkyl substances. Retrieved from https://www.canada.ca/en/health-canada/services/publications/healthy-living/objective-drinking-water-quality-per-polyfluoroalkyl-substances.html

Cantoni, B., Turolla, A., Wellmitz, J., Ruhl, A. S., & Antonelli, M. (2021). Perfluoroalkyl substances (PFAS) adsorption in drinking water by granular activated carbon: Influence of activated carbon and PFAS characteristics. *Science of The Total Environment, 795*, 148821.

Chowdhury, S., & Saha, P. D. (2012). Fixed-bed adsorption of Malachite Green onto binary solid mixture of adsorbents: seashells and eggshells. *Toxicological & Environmental Chemistry, 94*(7), 1272-1282.

Chularueangaksorn, P., Tanaka, S., Fujii, S., & Kunacheva, C. (2014). Adsorption of perfluorooctanoic acid (PFOA) onto anion exchange resin, non-ion exchange resin, and granular-activated carbon by batch and column. *Desalination and Water Treatment, 52*(34-36), 6542-6548.

Crincoli, K. R., Jones, P. K., & Huling, S. G. (2020). Fenton-driven oxidation of contaminant-spent granular activated carbon (GAC): GAC selection and implications. *Science of The Total Environment, 734*, 139435.

Dirani, L., Ayoub, G. M., Malaeb, L., & Zayyat, R. M. (2024). A review on the occurrence of per-and polyfluoroalkyl substances in the aquatic environment and treatment trends for their removal. *Journal of Environmental Chemical Engineering*, 113325.

Directive. (2020). 2020/2184 of the European Parliament and of the Council of 16 December 2020 on the quality of water intended for human consumption. *Off J Eur Communities, 435*, L 435/431-L 435/459.

Domingo, J. L., & Nadal, M. (2019). Human exposure to per-and polyfluoroalkyl substances (PFAS) through drinking water: A review of the recent scientific literature. *Environmental research, 177*, 108648.

Fath, B. D., & Jorgensen, S. E. (2020). *Managing global resources and universal processes*: CRC Press.

Ferndahl, S. (2024). Removal efficiency of multiple per-and polyfluoroalkyl substances (PFAS) in groundwater at a landfill using granular activated carbon (GAC) and anion exchange (AIX) column tests. In.

Gaines, L. G. (2023). Historical and current usage of per-and polyfluoroalkyl substances (PFAS): A literature review. *American Journal of Industrial Medicine, 66*(5), 353-378.

Legislative Publication: Gazzetta Ufficiale della Repubblica Italiana – Serie Generale, (2023).

Gu, B., Mehlhorn, T. L., Liang, L., & McCarthy, J. F. (1996). Competitive adsorption, displacement, and transport of organic matter on iron oxide: I. Competitive adsorption. *Geochimica et cosmochimica acta, 60*(11), 1943-1950.

Habib, Z., Song, M., Ikram, S., & Zahra, Z. (2024). Overview of per-and polyfluoroalkyl substances (PFAS), their applications, sources, and potential impacts on human health. *Pollutants, 4*(1), 136-152.

Hong, S., Kim, O.-J., Jung, S. K., Jeon, H. L., Kim, S., & Kil, J. (2024). The Exposure Status of Environmental Chemicals in South Korea: The Korean National Environmental Health Survey 2018–2020. *Toxics, 12*(11), 829.

Jais, F. M., Ibrahim, M. S. I., El-Shafie, A., Choong, C. E., Kim, M., Yoon, Y., & Jang, M. (2024). Updated review on current approaches and challenges for poly-and perfluoroalkyl substances removal using activated carbon-based adsorbents. *Journal of Water Process Engineering, 64*, 105625.

Ji, J. (2024). Taiwan Drafts Standards for PFAS in Drinking Water. Retrieved from https://sustainability.chemlinked.com/news/taiwan-drafts-standards-for-pfas-in-drinking-water

Kempisty, D. M., Arevalo, E., Spinelli, A. M., Edeback, V., Dickenson, E. R., Husted, C., . . . Knappe, D. R. (2022). Granular activated carbon adsorption of perfluoroalkyl acids from ground and surface water. *AWWA Water Science, 4*(1), e1269.

Kirsch, P. (2006). *Modern fluoroorganic chemistry: synthesis, reactivity, applications*: John Wiley & Sons.

Kozisek, F., Dvorakova, D., Kotal, F., Jeligova, H., Mayerova, L., Svobodova, V., . . . Pulkrabova, J. (2025). Assessing PFAS in drinking water: Insights from the Czech Republic's risk-based monitoring approach. *Chemosphere, 370*, 143969.

Krafft, M. P., & Riess, J. G. (2015). Selected physicochemical aspects of poly-and perfluoroalkylated substances relevant to performance, environment and sustainability—Part one. *Chemosphere, 129*, 4-19.

Kumara, M. K., & Bhattacharyya, D. (2022). Per-and poly-fluoroalkyl substances (PFASs) in drinking water and related health effects. In *Current Developments in Biotechnology and Bioengineering* (pp. 71-103): Elsevier.

Lee, J. C., Smaoui, S., Duffill, J., Marandi, B., & Varzakas, T. (2025). Research progress in current and emerging issues of PFASs' global impact: long-term health effects and governance of food systems. *Foods, 14*(6), 958.

Legislative Decree 6 July 2016, No. 122: Transposition of EU Directive 2014/80/EU amending Annex II of Directive 2006/118/EC. (2016). Gazzetta Ufficiale Retrieved from https://www.gazzettaufficiale.it/eli/id/2016/08/06/16G00142/sg

Leung, S. C. E., Wanninayake, D., Chen, D., Nguyen, N.-T., & Li, Q. (2023). Physicochemical properties and interactions of perfluoroalkyl substances (PFAS)-Challenges and opportunities in sensing and remediation. *Science of The Total Environment, 905*, 166764.

Li, D., Lee, C.-S., Zhang, Y., Das, R., Akter, F., Venkatesan, A. K., & Hsiao, B. S. (2023). Efficient removal of short-chain and long-chain PFAS by cationic nanocellulose. *Journal of Materials Chemistry A, 11*(18), 9868-9883.

Liu, Z., Peldszus, S., Sauvé, S., & Barbeau, B. (2024). Enhanced removal of trace-level per-and polyfluoroalkyl substances (PFAS) from drinking water using granular activated carbon (GAC): The role of ozonation. *Chemosphere, 368*, 143758.

Liu, Z., Yang, F., Zhai, T., Yu, J., Wang, C., Liu, Z., . . . Yang, M. (2024). Removal of PFOA from water by activated carbon adsorption: Influence of pore structure. *Journal of Environmental Chemical Engineering, 12*(5), 113923.

Lyu, Y., Brusseau, M. L., Chen, W., Yan, N., Fu, X., & Lin, X. (2018). Adsorption of PFOA at the air–water interface during transport in unsaturated porous media. *Environmental Science & Technology, 52*(14), 7745-7753.

McCleaf, P., Englund, S., Östlund, A., Lindegren, K., Wiberg, K., & Ahrens, L. (2017). Removal efficiency of multiple poly-and perfluoroalkyl substances (PFASs) in drinking water using granular activated carbon (GAC) and anion exchange (AE) column tests. *Water research, 120*, 77-87.

Murray, C. C., Marshall, R. E., Liu, C. J., Vatankhah, H., & Bellona, C. L. (2021). PFAS treatment with granular activated carbon and ion exchange resin: Comparing chain length, empty bed contact time, and cost. *Journal of Water Process Engineering, 44*, 102342.

Nakazawa, Y., Kosaka, K., Yoshida, N., Asami, M., & Matsui, Y. (2023). Long-term removal of perfluoroalkyl substances via activated carbon process for general advanced treatment purposes. *Water research, 245*, 120559.

National Academies of Sciences, E., & Medicine. (2022). *Guidance on PFAS exposure, testing, and clinical follow-up*.

Niarchos, G., Ahrens, L., Kleja, D. B., & Fagerlund, F. (2022). Per-and polyfluoroalkyl substance (PFAS) retention by colloidal activated carbon (CAC) using dynamic column experiments. *Environmental Pollution, 308*, 119667.

Ochoa-Herrera, V., & Sierra-Alvarez, R. (2008). Removal of perfluorinated surfactants by sorption onto granular activated carbon, zeolite and sludge. *Chemosphere, 72*(10), 1588-1593.

Pan, L., Cao, Y., Zang, J., Huang, Q., Wang, L., Zhang, Y., . . . Xie, Z. (2019). Preparation of iron-loaded granular activated carbon catalyst and its application in tetracycline antibiotic removal from aqueous solution. *International Journal of Environmental Research and Public Health, 16*(13), 2270.

Legge regionale 19 ottobre 2021, n. 25: Legge annuale di riordino dell'ordinamento regionale anno 2021, (2021).

Rahman, M. F., Peldszus, S., & Anderson, W. B. (2014). Behaviour and fate of perfluoroalkyl and polyfluoroalkyl substances (PFASs) in drinking water treatment: A review. *Water research, 50*, 318-340.

Riegel, M., Haist-Gulde, B., & Sacher, F. (2023). Sorptive removal of short-chain perfluoroalkyl substances (PFAS) during drinking water treatment using activated carbon and anion exchanger. *Environmental Sciences Europe, 35*(1), 12.

Senevirathna, S., Tanaka, S., Fujii, S., Kunacheva, C., Harada, H., Ariyadasa, B., & Shivakoti, B. (2010). Adsorption of perfluorooctane sulfonate (n-PFOS) onto non ion-exchange polymers and granular activated carbon: Batch and column test. *Desalination, 260*(1-3), 29-33.

Senevirathna, S., Tanaka, S., Fujii, S., Kunacheva, C., Harada, H., Shivakoti, B. R., & Okamoto, R. (2010). A comparative study of adsorption of perfluorooctane sulfonate (PFOS) onto granular activated carbon, ion-exchange polymers and non-ion-exchange polymers. *Chemosphere, 80*(6), 647-651.

Siriwardena, D. P., Crimi, M., Holsen, T. M., Bellona, C., Divine, C., & Dickenson, E. (2019). Influence of groundwater conditions and co-contaminants on

sorption of perfluoroalkyl compounds on granular activated carbon. *Remediation Journal, 29*(3), 5-15.

Steenland, K., Jin, C., MacNeil, J., Lally, C., Ducatman, A., Vieira, V., & Fletcher, T. (2009). Predictors of PFOA levels in a community surrounding a chemical plant. *Environmental health perspectives, 117*(7), 1083-1088.

Tang, Z. W., Hamid, F. S., Yusoff, I., & Chan, V. (2023). A review of PFAS research in Asia and occurrence of PFOA and PFOS in groundwater, surface water and coastal water in Asia. *Groundwater for Sustainable Development, 22*, 100947.

Umejuru, E. C., Street, R., & Edokpayi, J. N. (2024). A Comprehensive Review of the Occurrence, Distribution, Characteristics and Fate of Per-and Polyfluoroalkyl Substances in the African Continent. *Chemistry Africa, 7*(8), 4089-4103.

Valalamontes, A., & Adamopoulos, I. (2025). The Impact of PFAS on the Public Health and Safety of Future Food Supply in Europe: Challenges and Sustainable Solutions.

Vestergren, R., Cousins, I. T., Trudel, D., Wormuth, M., & Scheringer, M. (2008). Estimating the contribution of precursor compounds in consumer exposure to PFOS and PFOA. *Chemosphere, 73*(10), 1617-1624.

Wei, X., Shao, M., Du, L., & Horton, R. (2014). Humic acid transport in saturated porous media: Influence of flow velocity and influent concentration. *Journal of Environmental Sciences, 26*(12), 2554-2561.

Westreich, P., Mimna, R., Brewer, J., & Forrester, F. (2018). The removal of short-chain and long-chain perfluoroalkyl acids and sulfonates via granular activated carbons: A comparative column study. *Remediation Journal, 29*(1), 19-26.

Yuan, J., Mortazavian, S., Passeport, E., & Hofmann, R. (2022). Evaluating perfluorooctanoic acid (PFOA) and perfluorooctanesulfonic acid (PFOS) removal across granular activated carbon (GAC) filter-adsorbers in drinking water treatment plants. *Science of The Total Environment, 838*, 156406.

Yuan, W., Liu, Q., Song, S., Lu, Y., Yang, S., Fang, Z., & Shi, Z. (2023). A climate-water quality assessment framework for quantifying the contributions of climate change and human activities to water quality variations. *Journal of Environmental Management, 333*, 117441.

Zeng, C., Atkinson, A., Sharma, N., Ashani, H., Hjelmstad, A., Venkatesh, K., & Westerhoff, P. (2020). Removing per-and polyfluoroalkyl substances from

groundwaters using activated carbon and ion exchange resin packed columns. *AWWA Water Science, 2*(1), e1172.

Zhang, Y., Thomas, A., Apul, O., & Venkatesan, A. K. (2023). Coexisting ions and long-chain per-and polyfluoroalkyl substances (PFAS) inhibit the adsorption of short-chain PFAS by granular activated carbon. *Journal of hazardous materials, 460*, 132378.